HHS Public Access

Author manuscript

Biomaterials. Author manuscript; available in PMC 2017 October 01.

Published in final edited form as:

Biomaterials. 2016 October ; 104: 87–103. doi:10.1016/j.biomaterials.2016.06.050.

Superhydrophobic Materials for Biomedical Applications

Eric J. Falde[1], **Stefan T. Yohe**[1], **Yolonda L. Colson**[2], and **Mark W. Grinstaff**[1,*]

[1]Departments of Biomedical Engineering, Chemistry and Medicine, Boston University, 590 Commonwealth Avenue, Boston, MA 02215.

[2]Division of Thoracic Surgery, Department of Surgery Brigham and Women's Hospital, Boston, MA 02115

Abstract

Superhydrophobic surfaces are actively studied across a wide range of applications and industries, and are now finding increased use in the biomedical arena as substrates to control protein adsorption, cellular interaction, and bacterial growth, as well as platforms for drug delivery devices and for diagnostic tools. The commonality in the design of these materials is to create a stable or metastable air state at the material surface, which lends itself to a number of unique properties. These activities are catalyzing the development of new materials, applications, and fabrication techniques, as well as collaborations across material science, chemistry, engineering, and medicine given the interdisciplinary nature of this work. The review begins with a discussion of superhydrophobicity, and then explores biomedical applications that are utilizing superhydrophobicity in depth including material selection characteristics, *in vitro* performance, and *in vivo* performance. General trends are offered for each application in addition to discussion of conflicting data in the literature, and the review concludes with the authors' future perspectives on the utility of superhydrophobic surfaces for biomedical applications.

Keywords

Superhydrophobic; Biomaterials; Polymers; Drug Delivery; Tissue Engineering; Diagnostics; High Throughput Assays

1. Introduction

Superhydrophobic materials maintain air at the solid-liquid interface when in contact with water. These surfaces possess high apparent contact angles, by definition exceeding 150°, as a result of the composite solid-air surface formed under a water droplet (**Figure 1a**). An

Correspondence to: Eric J. Falde; Stefan T. Yohe.

[*]**Corresponding Author** mgrin@bu.edu, phone: (617) 358-3429, fax: (617) 358-3186.

Author Contributions

E.F., S.Y., Y.L.C. and M.W.G. wrote the manuscript. All authors reviewed the manuscript. All authors have given approval to the final version of the manuscript.

additional stipulation sometimes included in the superhydrophobic definition, depending on the application, is a low roll-off angle [1]. Cassie and Baxter are credited with first reporting the basis of superhydrophobicity in 1944 [2], expanding on the work by Wenzel in 1936 [3]. They demonstrated that porous hydrophobic surfaces exhibit high apparent contact angles compared to chemically equivalent flat substrates because of the maintenance of air at this interface. The very rough, hydrophobic substrate affords a partially wetted initial state, with a large air-water surface area, which serves as an energetic barrier that stabilizes the air. Cassie and Baxter specifically studied this effect in order to understand the water repellency of natural and synthetic clothing, and showed that porous, wax-covered textiles exhibit high apparent contact angles. They went on to discuss the roughness of feathers and fur and the resultant water repellent properties. Superhydrophobicity is a property of many naturally occurring substrates including plant leaves [4–8], many insect features including wings, legs, and eyes [9–16], feathers [17,18], fur [19], and beetle shells [20] (**Figure 1b**). Superhydrophobicity on these natural surfaces leads to improved function by providing water repellency or alternatively providing a self-cleaning surface where debris and pathogens are removed as water contacts and subsequently rolls off the surface. For example, dragonflies in the order *Odonata* possess a rough, fractal structure on their wings that aids in cleaning and preventing water adherence which inhibits flight [21]. A significant body of research now exists documenting that natural and biomimetic superhydrophobic surfaces exhibit low drag, self-cleaning, and/or non-fouling behaviors [21–25].

Synthetic superhydrophobic surfaces are being fabricated to harness these favorable surface properties, where surface chemistry and morphology are tailored to maintain air at the material-water interface. Materials used to produce superhydrophobic surfaces possess intrinsically low surface energy due to non-polar chemistries (i.e., CH_2/CH_3 or CF_2/CF_3) and close packed, stable atomic structures, resulting in high contact angles (up to 120°) even without material roughening. These low energy materials are either coated onto an already rough material, termed a “bottom-up” fabrication method, or are directly processed to induce roughness, termed “top-down” methods such as lithography. Examples of bottom-up methods include chemical deposition, assemblies of colloids, layer-by-layer methods, electrospraying, and electrospinning. Chemical deposition, for example, would coat an already rough substrate and impart superhydrophobicity [26]. Several in-depth reviews are available which focus on the materials and methods used to produce superhydrophobic surfaces, and interested readers are referred to these articles [27–35]. Other reviews concentrate on specific applications for superhydrophobic materials including anti-icing and corrosion resistance [36,37], high slip surfaces for watercraft [38–40], enhancement of evaporation and condensation processes [41–43], and switchable wettability [44–46].

This review focuses on the utility and development of superhydrophobic materials for biomedical applications, defined as those where the superhydrophobic surface interacts with tissues, cells, biological fluid, and/or biological molecules. There is significant interest in this area,[47–52] and we contextualize the results from previous research efforts, note general trends, and highlight recent and novel work using superhydrophobic surfaces, for example, in drug delivery and diagnostic devices. A brief thermodynamic framework is first presented for why superhydrophobicity exists in order to better understand the necessary

design parameters that are used for tailoring air stability at a material surface. Next, we discuss the biomedical applications employing superhydrophobic surfaces, including cell scaffolds, non-fouling surfaces to prevent binding of protein, cells, and/or bacteria, medical diagnostics, and drug delivery, as depicted in **Figure 2**. These include general principles, successes, and failures in these applications based on currently available research. Finally, the review concludes with remarks on the overall relevance of superhydrophobic surfaces in biomedical applications, and future directions and research opportunities for superhydrophobic materials.

2. Contact Angle, Superhydrophobicity, and Long-term Air Stability

The Wenzel and Cassie-Baxter models are the conventional descriptions of wetting states on a rough material. Both models are derived from the Young's equation, given by:

$$\cos\theta = \frac{\gamma_{SV} - \gamma_{SL}}{\gamma_{LV}}$$

where γ is the interfacial surface energy between the solid-vapor (SV), solid-liquid (SL), or liquid-vapor (LV) phases. The measured angle in the Young's equation, θ, is referred to as the contact angle (CA) of a surface, or the Young's angle. The contact angle of a surface is a measure of the equilibrium of the surface energy of these three interfaces on a *flat* material surface. Most often, contact angles are measured using water as the liquid phase. By definition, flat materials with CA > 90° in contact with water are referred to as hydrophobic, whereas materials with CA < 90° are referred to as hydrophilic, as shown in **Figure 1a**. Large contact angles (hydrophobic) imply that γ_{SL} is large (high energy interface, “unfavored” water-material interface), whereas small contact angles (hydrophilic) imply γ_{SL} is small (low energy interface, “favored” water-material interface).

Contact angle measurements are performed both statically and dynamically. Measuring the static contact angle of a surface involves placing a droplet of water on the surface with no further manipulation, with a resultant CA close to the equilibrium predicted by Young's equation. As the name implies, dynamic contact angle measurements are those measured as the droplet size changes, both where volume is being added to the droplet (advancing CA), or where volume is being removed (receding CA). The advancing CA is a measure of how energetically favorable it is for a surface to wet, whereas the receding contact angle is a measure of how favorable for a surface to de-wet. The difference between the advancing and receding contact angle is referred to as contact angle hysteresis [53,54]. Higher hysteresis is a sign that intermediate wetting states resist de-wetting by ‘pinning’ the contact line. Since a static CA can take any value between the advancing and receding CAs, the latter measurements are more reliable [55].

The Wenzel and Cassie-Baxter models utilize Young's equation and extend it to *rough* material surfaces. The Wenzel model [3] states the following:

$$\cos\theta^* = r\cos\theta$$

where θ is the Young's angle, r is a roughness factor or roughness coefficient, and θ^* is the apparent or measured contact angle on a rough surface, as shown in **Figure 1**. The roughness factor is the ratio between (1) the surface area a droplet contacts on the rough surface and (2) the surface area the droplet *would have* contacted on a chemically equivalent flat surface. An r = 1 implies the surface is smooth, where an r > 1 implies roughness features. The Wenzel model predicts that both apparent hydrophilicity and hydrophobicity are enhanced with roughness. Another result of this wetting state is also an increase in contact angle hysteresis; the increased roughness of the surface results in further droplet-material contact and pinning of the droplet during de-wetting.

At high roughness values (r ≈ 1.7), the increase in contact angle hysteresis, predicted by the Wenzel model, drops dramatically with hydrophobic surfaces [53,56–63]. Instead of completely wetting the surface, air is maintained under the droplet to prevent wetting. *This is the basis of superhydrophobicity.* The Cassie-Baxter model extends the Wenzel model to describe wetting of a surface where two phases are present under the applied droplet (**Figure 1)**. The Cassie-Baxter model [2] states the following:

$$\cos\theta^* = f_1 \cos\theta_1 + f_2 \cos\theta_2$$

where f_1 and f_2 (=1- f_1) are the surface fractions of phase 1 and phase 2, θ_1 and θ_2 are Young's contact angles for these two phases, and θ^* is the apparent contact angle on the material surface. One way of thinking about the Cassie-Baxter model is as a weighted average between the two phases, where f_1 and f_2 attribute a certain fraction of the surface area the droplet is contacting at the composite surface. The relationship is simplified for a superhydrophobic surface when air is the second phase under the applied droplet (θ = 180°):

$$\cos\theta^* = f\,(1+\cos\theta) - 1$$

where the Cassie angle is now a function of the fraction of solid (f) at the droplet interface and Young's angle of the solid (θ). Combined, the Wenzel model and Cassie-Baxter model provide a framework for understanding the complicated interplay between the three phase boundaries at a rough material surface.

It is often unclear for a given surface whether the Wenzel or Cassie-Baxter state is favored, or when the transition between the two states occurs with modification to surface roughness and/or surface energy [64–69]. Theoretical work is ongoing to identify appropriate boundary conditions between states, and remains an active area of research [70–73]. However, when examining the Cassie-Baxter equation, it is clear that both surface chemistry and surface roughness are the primary factors at play when determining the behavior of water, and droplets thereof, on a material surface.

As mentioned earlier, the most common definition of superhydrophobic surfaces describes those with apparent contact angles above 150°, where the “apparent” designation refers to a contact angle measurement taken on a rough material surface. Other researchers choose to further limit the designation of superhydrophobicity to materials which exhibit contact angle

hysteresis <5°, as low hysteresis is an important property in applications such as self-cleaning and low-drag surfaces. While these designations are valuable benchmarks, they are also arbitrary as no special air layer stability is conferred at these values. Empirical studies by Cohen [68] and Quéré [64] are good examples where boundaries of the stable Cassie-Baxter state for a specific superhydrophobic system are explored and identified, and which ultimately provides a better description of superhydrophobicity. Additionally, measuring the underwater stability of superhydrophobic surfaces is valuable for accurately predicting air layer stability and wetting state. Rather than apply a single droplet to a superhydrophobic surface and measure the instantaneous contact angle, underwater stability assays instead apply a "continuum" of droplets on a superhydrophobic surface by submersion in water over a period of time. Air content can be qualitatively or quantitatively measured using a number of different techniques including the reflection of light [74,75], clinical ultrasound [76], 3D x-ray imaging [77,78], oxygen sensing [14], and fluid dynamics [79–82]. Empirical results and theoretical studies show that the air layer at a material surface can be metastable or stable with a dependence on the intrinsic material surface energy, fill fraction, aspect ratio/geometry, and reentrant curvature [68,74,83–88].

It is also noteworthy that a stable Cassie-Baxter state is relative to the applied conditions, where a sufficient "treatment" with vibration, acoustic pressure, hydraulic pressure, or changes in surface energy will force the Wenzel state of wetting by removing the air layer [89–92]. Environmental conditions such as the presence of proteins and biological surfactants are specifically relevant for the biomedical applications discussed in this review, as it is well established that "bio-fouling" affects the longevity of the trapped air layer [93–95]. However, regardless of conditions, higher apparent contact angles are still generally predictive of increased stability of a superhydrophobic surface [96,97].

3. Protein Adsorption to Superhydrophobic Biomaterials

Controlling protein adsorption to a biomaterial surface, whether inhibiting adsorption entirely or selectively adsorbing protein is of significant importance for many applications discussed in this review, from bacterial and cellular interactions to diagnostic and drug delivery platforms. Designing a biomaterial surface that avoids all protein adsorption has been elusive due to the large number of proteins *in vivo* and their structural and physio-chemical diversity [98–100]. In general, hydrophilic patches on the surface of proteins interact with a hydrophilic biomaterial surface with minimal subsequent denaturing/unfolding of the protein. Historically, it was thought that hydrophobic surfaces would suppress adsorption of proteins, as the hydrophobic residues of a protein are sequestered within the folded three-dimensional structure. However, we now know that hydrophobic materials readily adsorb proteins, either by direct interactions of hydrophobic patches on the protein surface or through denaturing, thereby exposing the buried hydrophobic residues and allowing the protein to bind the material surface. Surface binding of the protein is favored both enthalpically via the creation of new interactions between the surface and the protein, and entropically via the increased number of possible states that the water can reside. Hydrophilic surfaces more often have less stably-bound proteins and as a consequence exhibit higher protein turnover at the material surface.

There are two general strategies to reduce or prevent unwanted protein adsorption at biomaterial surfaces: fabricating a surface that is completely non-fouling, or allowing the adsorption of specific proteins to the material surface. Considering non-fouling surfaces first, the most successful strategy grafts a large number of “loose” hydrophilic polymer chains off of a material surface. The most widely used polymer for this strategy is poly(ethylene glycol) (PEG) [101–106], although similar flexible polymer chains, self-assembled monolayers (SAMs), polysaccharides, proteins, and many other materials have been explored [107–113]. These flexible polymer chains form a brush structure at the material surface and swell due to their hydrophilicity, thereby trapping water at the material interface. If a protein binds to this interface, compression of this hydrogel-like structure occurs (unfavored entropically) as the polymer chains are confined at the material interface and forced into an unfavorable compressed/globular confirmation with expulsion of water molecules to the surrounding. These energy barriers exceed the enthalpy term assocaited with protein adsorption to the surface. This strategy is extensively studied and is used for a number of macroscopic material surfaces as well as many nanoparticle/microparticle designs for prolonged systemic circulation.

The limited surface chemistries and architectures available for non-fouling surfaces led others to investigate surfaces designed to bind a specific protein or set of proteins [114–117]. Non-specific protein adsorption is suppressed while specific protein adsorption is promoted in order to generate a more defined biological response. Most often short peptide sequences or full proteins are grafted to the material surface, and the exposed sequences inhibit further biological activity at the surface [118]. The location of the device also impacts which proteins are most appropriate for use. For example, preventing the binding of thrombin and fibrinogen is critical in the prevention of thrombus formation at blood-contacting devices.

Texturing a material surface with micro- and/or nano-scale architecture is a complementary approach explored to control protein adsorption at a biomaterial surface. Protein adsorption can be tuned by fabricating a material with appropriate surface roughness or curvature [119–124]. For example, Roach *et al.* [120] showed that the surface curvature can dictate whether a protein will bind as well as what confirmation it will adopt when bound. For example, silica particles of varying sizes (15 - 165 nm) were produced, resulting in a high, but less than 150° contact angle where smaller particles were able to suppress some protein binding. Albumin, a globulin protein, is stabilized by this surface curvature, whereas fibrinogen, a rod-like protein, is distorted at the surface and distended over particles with higher surface curvature. Mandal *et al.* [121] showed similar findings in their work, where changing the curvature of a surface led to conformational changes in 15 different peptides. A limitation to this approach is that each material's architecture tested only prevented a subset of proteins from binding. With the diversity of proteins present in the biologic milieu, it is unclear whether a generic surface roughness could prevent all proteins from binding. While significant empirical knowledge exists with regard to protein binding to biomaterials, further development of structure-property relationships are warranted and represent an ongoing and active area of research [125].

The use of superhydrophobic surfaces for preventing protein adsorption utilizes a unique strategy to those previously mentioned through maintenance of an air layer at the material

surface. This air layer at the interface limits the available water-material surface area and decreases the total area available for protein binding. This is the first step in biofouling, the prevention of which has been the subject of multiple reviews [84,126,127]. Work by Leibner *et al.* [128] nicely contextualizes the use of superhydrophobic surfaces for biomedical applications, and the conflicting design criteria that are required for their use. Their work focused on the adsorption of human serum albumin to commercially available expanded polytetrafluoroethylene (ePTFE). When entrapped air is maintained within the highly hydrophobic ePTFE matrix, little or no adsorption of albumin from phosphate buffered saline (PBS) is detected on the material surface. However, when air is removed from the ePTFE material, albumin is adsorbed to the entire material surface, including the portion of the surface that once housed air. Huang *et al.* [129] showed similar results, where a templated superhydrophilic-superhydrophobic structure comprised of TiO_2 nanotubes exhibited suppression of protein binding when air is present in the superhydrophobic regions. Removal of the air layer increases protein binding, as shown in **Figure 3**. Work by both sets of authors demonstrates that superhydrophobic surfaces support an entrapped air layer to initially prevent protein binding, but removing the air "reveals" a high surface area material that adsorbs larger quantities of protein to the surface.

Moreover, proteins and other biological surfactants can themselves promote air removal from the superhydrophobic surfaces in two ways. Proteins are surface-active molecules (surfactants) that decrease the interaction energy at the material-water interface through reduction of the surface tension of water. Further, proteins will adsorb to the low energy material surface over time with denaturing-and-binding events, thereby increasing the surface energy of the material to favor the interaction with water. This is shown conceptually in **Figure 4** where water infiltration is promoted with further protein binding. Accardo *et al.* [130] compared the effects of water and water-lysozyme solutions on microfabricated poly(methyl methacrylate) (PMMA) pillars. The rough PMMA surface showed significant droplet pinning with the presence of lysozyme in the water solution. This water pinning indicates movement of water into the interstices of the pillars and formation of a "hybrid" state between the wetting Wenzel state and the non-wetting Cassie-Baxter state. Without the presence of lysozyme, no droplet pinning occurred at the surface. Choi *et al.* [131] studied the evaporation of a protein-containing solution on needle-like, nano-structured superhydrophobic surfaces. The apparent contact angle of these surfaces is between 111° and 165° depending on needle height and pitch. All contact angle measurements of the surfaces showed a decrease to nearly 0° over 3 hours (i.e., complete adsorption and movement towards the Wenzel state) when using media that contained 10% fetal bovine serum. Protein binding to the surface promoted penetration into the surface roughness features, which is also confirmed by a strong observable pinning effect. Superhydrophobic nano-structured surfaces with higher apparent contact angles prevented adsorption and a change in contact angle for longer periods. Without proteins and serum in solution, water is no longer pinned to the superhydrophobic surfaces and only exhibited the non-wetted Cassie-Baxter state.

Superhydrophobic surfaces produce a composite surface of a hydrophobic material and entrapped air that effectively reduces protein binding as protein cannot bind the air-liquid

interface. However, this effect is transient since proteins will eventually bind the areas on the material surface regardless of its chemistry and surface energy, which slowly leads to wetting of this surface and eventual displacement of the air layer. This leads to a subsequent significant increase in effective surface area for protein binding compared to a flat material surface, allowing substantial amounts of protein to adsorb. These conflicting design criteria aside, superhydrophobic surfaces can effectively inhibit or prevent protein binding. Perry *et al.* [132] quantified the amount of fibrinogen and albumin adsorption on porous silica coatings with different self-assembled monolayers, creating both superhydrophobic and superhydrophilic surfaces. When the superhydrophobic surfaces are exposed to protein containing solutions, less total protein binding occurs compared to the superhydrophilic surfaces. It is noteworthy that if the superhydrophobic surface is rendered non-superhydrophobic, the increased surface area of this material leads to more protein binding compared to the superhydrophilic surface. Zhai *et al.* [133] used a micropatterning technique to construct a synthetic mimic of the Namib Beetle, where they produced a superhydrophobic surface patterned with superhydrophilic regions. Polyelectrolytes and dyes selectively adsorbed to the superhydrophilic regions while the superhydrophobic regions remained protected.

The use of surface curvature is a promising approach to prevent protein binding on superhydrophobic surfaces as reviewed by Lord *et al.* [134]. For example, Koc *et al.* [123] fabricated superhydrophobic surfaces using both a sol-gel deposition process and copper oxidation to form nanoneedles. These surfaces are subsequently chemically modified to afford hydrocarbon or fluorocarbon coated surfaces. Superhydrophobic surfaces with large roughness features (4 μm, 800 nm) adsorb more bovine serum albumin (BSA) than chemically equivalent flat surfaces, whereas surfaces with small roughness features (10 nm) adsorb much less. The authors state that with nano-scale roughness adsorption may still occur, but the sharp curvature of the surface prevents a stable binding event. When the surfaces are under high shear, less protein adsorption occurs. Further, Kurylowicz et al. [135] showed that as surface curvature increased, the number of protein dimers and higher order aggregates decreased. The authors use polystyrene (PS) surfaces, either flat or with adsorbed nanoparticles that are 50 or 27 nm in diameter, and employ single-molecule force microscopy to show that lactalbumin and lactoglobulin are more closely packed on the flat than highly curved surfaces.

Superhydrophobic surfaces effectively limit the amount of surface area available for proteins to bind with the presence of a protective air barrier. However, this strategy is restrictive in that the hydrophobic, rough materials necessary to produce the superhydrophobic effect are also known to adsorb proteins reducing the longevity of this barrier. The initial maintenance of air at the material surface reduces protein adsorption but the surfactant properties of proteins eventually lead to loss of the air layer and an increase in the amount of protein that binds. The required time for the air layer to be present at the surface is an important consideration for the corresponding suppression of protein binding and the surface's intended application.

4. Cellular Interactions

Similar to protein binding, the presence of entrapped air modifies cell-material surface interactions, and additionally influences cell proliferation and growth. As discussed in the previous section, protein binding occurs (rapidly) and this protein coated surface affects cell binding. Ballester-Beltrán *et al.* [136] examined the binding of fibronectin (FN) to superhydrophobic surfaces, and subsequently evaluated cell binding to these surfaces. Superhydrophobic porous PS surfaces are produced using phase-inversion. The authors found that limited quantities of FN bind superhydrophobic PS surfaces compared to flat PS and glass surfaces. Further, superhydrophobic PS surfaces caused FN to adsorb to the surface differently, as indicated by results from both an ELISA assay and MC3T3-E1 cultured cells that produced fewer mature focal adhesions. Superhydrophobic surfaces exhibited fewer bound cells compared to control surfaces, which showed extensive cell binding and cellular projections. Cells that bind superhydrophobic surfaces form a round morphology with few cellular projections. After several days of incubation and growth, cell contractility, reorganization of FN at the cell surface, and cell proliferation are all reduced on superhydrophobic surfaces compared to nonsuperhydrophobic surfaces. Alves *et al.* [137] produced flat poly(L-lactic acid) (PLLA) surfaces cast from dioxane, and superhydrophobic surfaces from an additional dip treatment in ethanol. Rat bone marrow derived cells cultured for 1, 3, 7, and 21 days on these surfaces result in minimal cell growth and spreading on the superhydrophobic surfaces at all time points. Wang *et al.* [138] fabricated 50 μm pillars of SU-8 on glass slides with subsequent silane functionalization. Cells plated on these superhydrophobic surfaces for 72 hours remained at the top of the pillars, and the stable air layer prevents growth in the well regions between pillars (**Figure 4**). In contrast, without silane functionalization, cells grow everywhere on the surfaces as water can contact the entire surface (Wenzel state). The entrapped air layer at superhydrophobic surfaces is stable up to 4 months in cell culture, but is lost when exposed to a low surface tension 1:1 water:ethanol or sufficient pressure.

The roughness and curvature of a superhydrophobic surface can also inhibit cell growth after binding, as reviewed by Lord *et al.* [134]. Di Mundo *et al.* [139] studied how an osteoblast cell line (Saos2) responded to different roughness and densities of nanometer-sized dots. A decrease in cell adhesion is observed with increased roughness level (decrease in nanodot size). Additionally, after initial cell binding, growth is inhibited on the rougher, superhydrophobic surfaces. The authors hypothesized that superhydrophobic surfaces are more “nanometric” and prevented protein and cellular binding. The increase in nanodot curvature also prevented cell filopodia-material interactions. The authors make no direct mention of air being maintained at the surface leading to this effect, but this is plausible based on the geometry of the fabricated surfaces. Cell density is twice as high on flat surfaces compared to superhydrophobic ones composed of the same material. Ranella *et al.* [140] tuned cell adhesion by controlling the roughness on superhydrophobic 3D micro/nano silicon structures. Increasing the roughness and superhydrophobicity of the surfaces decreased 3T3 cell viability and diminished their ability to spread on the surface. Bauer *et al.* [141] fabricated vertically oriented TiO_2 nanotubes with defined diameters between 15 and 100 nm, and coated them with octadecylphosphonic acid to produce surfaces with apparent

contact angles between 102° and 167°. Unmodified surfaces are “superhydrophilic” and completely wet in contact with water. Cells incubated on the superhydrophobic surfaces of any TiO_2 nanotube diameter for 24 hours showed the same amount of binding compared to control surfaces. However, after 24 hours, the air present at superhydrophobic surfaces prevented further growth compared to superhydrophilic and control surfaces. Additionally, superhydrophobic surfaces composed of 15 nm features exhibited more collagen and less albumin binding over 24 hours when compared to surfaces of 100 nm tubes. The authors postulated that the very high curvature at the surface influences the type of proteins that bind (i.e., rod shaped protein vs. globular protein) and, thus, cell binding. Dowling *et al.* [142] fabricated PS surfaces with apparent contact angles of 12° to 155°, and RMS roughness of 19 to 2365 nm. Nonsuperhydrophobic surfaces showed 90% more MG63 cells bound than on superhydrophobic substrates. Proliferation of cells is low on both the non-superhydrophobic and superhydrophobic surfaces.

An active area of research is spatially controlled growth of cells through patterned superhydrophobic-hydrophilic substrates. This methodology is used for labon-a-chip diagnostic applications (discussed later), or alternatively applied to other applications such as tissue engineering constructs. Oliviera *et al.* [143] produced patterned superhydrophobic PS surfaces by a phase separation method, and studied the growth of three cells lines (SaOs-2, L929, and ATDC5). Produced by UVO irradiation treatment, cell growth is selectively seen on hydrophilic spots, and in most cases cell binding and growth is suppressed over 6 days of cell culture on superhydrophobic regions. Ishizaki *et al.* [144] fabricated a micropatterned superhydrophobic and superhydrophilic surface using chemical vapor deposition (CVD). Patterns of UV treatment afforded superhydrophilic regions (-OH and -COOH functional groups) while the trimethylmethoxysilane (TMMOS) treated areas exhibited superhydrophobicity. Mouse 3T3 cells incubated on the surfaces for 1 and 24 hours showed selective binding and growth on the superhydrophilic regions, as shown in **Figure 5a**. Piret *et al.* [145] cultured CHO cells on micropatterned superhydrophobic/superhydrophilic silicon nanowire arrays for 3 hours, with subsequent growth of cells for 48 hours. Superhydrophobic regions are produced on the arrays by using octadecyltrichlorosilane (OTS), with apparent contact angles of 160°. Binding and growth of CHO cells is completely suppressed on the superhydrophobic regions, with all binding occurring in the superhydrophilic regions. The bound cells exhibited cytoplasmic projections, which remained within the superhydrophilic regions. Huang *et al.* [129] used TiO_2 nanotubes coated with perfluorocarbons to produce superhydrophobicity, which are then removed by UV in selected areas to expose the superhydrophilic material below. The authors demonstrated that multiple cell type can be seeded specifically on the superhydrophilic sections when in FBS-supplemented media, but observed much less specificity when in protein-free basal media, even when wetted. After two days, the templated cells overgrow their original seeding patterns, highlighting the temporary utility of these patterns. Finally, the authors showed that this seeding can be achieved to the same extent whether or not air is present, suggesting that hydrophilic domains are naturally better sites for cell adherence. However, Efremov *et al.* [146] demonstrated the utility of the air layer maintenance during cell seeding. The authors used lithography to produce a surface with highly hydrophilic (CA of 17°) poly(2-hydroxyethyl methacrylate)-co-(ethylene

dimethacrylate) (HEMAEDMA) spots separated by thin (~50 μm) barriers of nearly superhydrophobic (advancing CA of 146°) pentafluoropropyl methacrylate. This enabled the seeding of adjacent spots with different cell types for 18 hours, after which the surface is wet completely to study cell-cell communication. Separation of the cell types in each spot is maintained for over 72 hours without overgrowth of the hydrophobic barriers, as shown in **Figure 5b**. Recent work by the Levkin group demonstrated maintenance of these micropatterns for 5 days of culture with a variety of cell lines as well as pipette-free medium exchange and drug screening assays [147]. The Mano group also used superhydrophobic surfaces to prepare cell spheroids [148]. Micro-scale indentations, which serve to pin aqueous droplets on an otherwise superhydrophobic PS, are used for housing fibroblast-like L929 cells in 5 μL of media. This surface is then inverted, and over 48 hours the cells in each droplet aggregate into a spheroid.

Lastly, in contrast to other findings, some authors found that superhydrophobic surfaces promoted cell growth. Senesi *et al.* [149] prepared “Teflon-like coatings” by depositing C_2F_4 gas in RF mode using a parallel plate chemical CVD, resulting in a rough fibular structure with apparent contact angles up to 160° and RMS roughness values of 524 nm. The rougher, more superhydrophobic substrates served as better 3T3 cell substrates over 96 hours than surfaces that are less rough. It should be noted that the SEM micrographs appeared to suggest that this air layer was unstable and was removed quickly: instead of preventing cell binding, an increased surface area would enhance cell binding and growth. Furthermore Gristina *et al.* [150] used these same coatings and incubation conditions but different cell types (NCTC 2544 keratinocytes, 3T3 fibroblasts, MG63 osteoblasts) to show similar results with rougher substrates affording increased viability, adhesion, and spreading with all three cell lines. Luo *et al.* [151] fabricated perfluoro-functionalized poly(3,4-ethylenedioxythiophene) (PEDOT) films using electrochemical polymerization in an ionic liquid, where PEDOT-OH films and smooth PEDOT films were used as controls. The authors showed that protein adsorption doubled on superhydrophobic PEDOT-F surfaces compared to PEDOT-OH substrates. In normal serum-supplemented media, P19 embryonal carcinoma cells exhibited the highest viability on rough superhydrophobic PEDOT-F substrates. In serum-free media, however, fewer cells adhered on both substrates, which the authors attributed to decreased protein adsorption.

Superhydrophobic surfaces, by maintaining air at the interface, reduce the effective area for cells to bind and cellular proliferation rates. In the work examined, air is used as a temporary barrier to cell growth with studies performed over relatively short time scales (hours to several days). However, as discussed in the previous section, the air barrier is eventually lost because of the surfactant properties of biomolecules, and highlights the need for further advances in materials and material properties to prolong the stability of the air layer for longer-term prevention of cell binding.

5. Blood Compatibility

There is significant demand for blood-compatible materials for many applications, including diagnostic platforms and prosthetic grafts to treat the increasing prevalence of peripheral vascular disease, coronary artery disease, and hemodialysis [152–154]. Protein binding,

activation of platelets, restenosis, and resultant formation of thrombi both on and downstream from biomaterial surfaces remain the primary technical/biological barriers for the success of these devices. Superhydrophobic surfaces are being explored for their potential use in increasing blood compatibility, where the gaseous interface provides a unique approach to prevent material-blood interactions. Toes *et al.* [155] studied commercial expanded polytetrafluoroethylene (ePTFE) and superhydrophobic ePTFE (modified commercial ePTFE using ion beam etching) as vascular grafts in mice to determine if superhydrophobicity led to improved performance. Early effects of the ePTFE and superhydrophobic ePTFE were studied by examining platelet glycoprotein IIIa, a receptor which mediates thrombus formation, after 15 minutes of contact with human blood in a circulation setup. Blood that contacted superhydrophobic ePTFE surfaces showed higher levels of glycoprotein IIIa expression, indicating that platelets are more activated compared to the commercially available ePTFE surface. Subjecting the grafts to direct circulation in a pig carotid artery for 28 days revealed no difference in the thickness of neointima formation between the nonsuperhydrophobic and superhydrophobic grafts (**Figure 6**). These findings are in direct contrast to those reported by Busscher *et al.* [156], who noted a significantly decreased neointima formation with the use of the superhydrophobic ePTFE surfaces compared to commercially available ePTFE surfaces.

Hou *et al.* reported successful prevention of platelet activation using superhydrophobic surfaces [157]. The authors generated a superhydrophobic, porous polypropylene (PP) surface using a solvent casting method. Upon exposing flat PP and the porous superhydrophobic PP surfaces to citrated blood and platelet rich plasma for 90 minutes, the authors observed significant numbers of adsorbed platelets on the flat PP, in contrast to superhydrophobic PP surfaces that adsorbed fewer adsorbed platelets. Additionally, fewer fused platelets and pseudopodia extensions are observed on the superhydrophobic PP surface.

Sun *et al.* [158] produced nanostructures of poly(carbonate urethane)s (PCUs) with fluorinated alkyl side chains by casting on top of an aligned carbon nanotube array. When the superhydrophobic PCUs structure is exposed to platelet rich plasma for 30 minutes with subsequent gentle rinsing, and minimal platelet adherence, activation, and deformation are observed. The smooth PCUs with contact angles of ≈110° showed greater platelet binding and deformation than the nanostructured PCUs. Additionally, superhydrophobic PCU surfaces gave less expression of the glycoprotein gpIIb/IIIa complex and PAC+/CD62+, showing reduction in both early and late stage platelet activation events. The authors state that the decrease in platelet activation at superhydrophobic surfaces is due to a decrease in protein adsorption and the presence of entrapped air.

Zhou *et al.* [159] fabricated polydimethylsiloxane (PDMS) with a textured surface by soft lithography. Significantly larger numbers of platelets adhered to flat PDMS surfaces compared to those with pillars after 60 minutes of exposure. Superhydrophobic surfaces only bind platelets on top of the PDMS pillars, and not the interior regions protected by air, and the least wettable surfaces bound the lowest number of platelets. Additionally, submicron grooves (“dual-scale roughness”) introduced onto the pillars further suppressed platelet adhesion. Similarly, Huang *et al.* [160] manufactured stainless steel with a layer of

TiO_2 nanotubes coated with perfluorooctyl-triethoxysilane (PTES) to impart superhydrophobicity. The authors reported a marked reduction in platelet adhesion over two hours on the superhydrophobic surfaces.

Nokes *et al.* [161] used a clever roll-to-roll shrink-induced manufacturing process to produce superhydrophobic plastics. Specifically, a polystyrene sheet is stretched and held while silver and calcium nanoparticles are added by thermal vapor deposition, after which the sheet is allowed to shrink back to shape, causing the stiff metallic layer to wrinkle. Both micro- and nano-scale roughness are observed on the surface and these surfaces can be used as a mold to emboss polypropylene (PP). The resulting PP exhibited a CA >150° and hysteresis <10° with both water and blood. The authors demonstrated blood drop roll-off and reduced coagulation compared to the flat PP surface over 50 minutes.

In general, superhydrophobic surfaces reduce platelet binding and activation *in vitro*. It is noteworthy that the two most stringent and demanding *in vivo* experiments using native and superhydrophobic ePTFE afforded conflicting results.

6. Bacterial Interactions

There are millions of device-related bacterial infections (>1M in the United States alone) each year. Based on data collected in the US, nosocomial infections account for half [162,163]. Infections are most commonly associated with cardiovascular implants (stents, heart valve replacements, central venous lines, etc.), where 7.4% of all implanted cardiovascular devices result in a bacterial infection. Orthopedic implants follow closely behind (hip and knee replacements, etc.), with 4.3% of all implants resulting in infection. Over 90% of implants retain pathogenic microorganisms when implanted, derived from a patient's skin, medical personnel clothing, medical equipment, or already present in the body, and prevention of infection remains a significant challenge [164,165].

Consequently, superhydrophobic surfaces are being pursued as antibacterial coatings to reduce infections using the entrapped air layer to inhibit adherence. Unlike many of the other applications discussed thus far, antibacterial suppression is necessary for a short duration after implantation. There is a critical period of hours-todays where bacterial binding and growth must be suppressed to allow cell and tissue integration to occur [166]. Many of the approaches employing superhydrophobic materials are reviewed by Zhang *et al.* and the reader is referred to this article [167]. Crick *et al.* [168] fabricated a superhydrophobic surface from a silicone elastomer using aerosol-assisted CVD. When compared to flat glass surfaces or flat silicone surfaces, counts of both *Escherichia coli* (*E. coli*) and Methicillin-resistant *Staphylococcus aureus* (*S. aureus*) are reduced after submersion in the bacterial broth for 1 hour. *S. aureus* showed significantly less growth on superhydrophobic surfaces (2.5-fold lower), and *E. coli* showed slightly less than either control (1.6-fold lower). Loss of air may account for the small amount of bacterial growth suppression observed. Tang *et al.* [169] used flat TiO_2 surfaces and calcined to form TiO_2 nanotubes, and coated both with perfluorooctyl-triethoxysilane (PTES) to form superhydrophobic and hydrophobic surfaces. The superhydrophobic surfaces resisted *S. aureus* adhesion compared to unmodified nanotubes and the flat hydrophilic titanium surfaces. Loo *et al.* [170] showed the delayed

growth of bacteria on polyvinyl chloride (PVC) endotracheal tubes with texturing of the surfaces. A rough microstructure PVC with micron-sized features is prepared using a controlled precipitation method via selection of appropriate solvent combinations. Smooth PVC surfaces showed *P. aeruginosa* binding within six hours and subsequent biofilm formation. With the superhydrophobic textured PVC surfaces, binding and biofilm production did not occur until 18 to 24 hours (**Figure 7**). After 96 hours, extensive growth is observed on all surfaces, with only a small amount of suppression on superhydrophobic surfaces. The authors state that the air layer at superhydrophobic surfaces is likely fully removed by 96 hours.

Ma *et al.* [171] demonstrated that the nanostructures on the Taro leaf, which impart superhydrophobicity, are responsible for its resistance to *P. aeruginosa* adhesion. They attribute this to the microstructures on the “papilla” which trap air at the surface and prevent binding. When the leaves are wetted with ethanol to completely remove the air layer, bacteria binding increased on the surface although the wax crystals present on the leaves still suppressed bacterial growth even when wetted. Epidermal cells between the wax crystals showed extensive growth with removal of the protective air layer. Pernites *et al.* [172] manufactured superhydrophobic surfaces by depositing PS particles on a surface with subsequent electropolymerization of conductive polythiophene on top to produce a rough superhydrophobic surface. Without an electric field, the films are resistant to fibrinogen and *E. coli* binding. When an electric field is used to remove the air layer (electrowetting), attachment of both fibrinogen and *E. coli* is enhanced.

Hasan *et al.* demonstrated that the wings of the cicada *Psaltoda claripennis* are superhydrophobic and inhibited growth of Gram-negative bacteria but not Gram-positive or mammalian cells [173]. However, the authors modeled this result as a biophysical effect of the surface topology and stiffness without including the effect of entrapped air [174], and demonstrated the same effect with hydrophilic materials of the same topology [175]. A superhydrophobic silicon surface with a similar nanopillar topology, manufactured using deep reactive ion etching by Hasan *et al.* [176], showed anti-bacterial activity against *E. coli* but not *S. aureus*, consistent with this mechanism. It should be noted that this seems to be a limited effect, as generally rougher surfaces increase bacterial adhesion and growth [177,178].

In addition to the intrinsic suppression of bacterial binding with an entrapped air layer at the surface, other researchers are exploring encapsulated antibacterial agents to further prevent bacterial growth at the surface and in the surrounding regions. Berendjchi *et al.* [179] employed silica sols doped with two different amounts of copper nanoparticles. Release of copper ions from fabrics impregnated with these nanoparticles resulted in a 72 to 99-fold reduction in *S. aureus* and *E. coli* growth compared to undoped silica, as well as suppression in bacterial growth in the surrounding culture. Both materials trapped air, and the release of copper from the substrate led to less bacterial growth on these materials. Xue *et al.* [180] decorated cotton textiles using silver nanoparticles. This treatment produced superhydrophobic cotton due to the roughness induced by adding silver nanoparticles to the surface. Compared to non-decorated cotton textiles, the decorated superhydrophobic textiles showed greater antibacterial activity against *E. coli*. Chung *et al.* [181] produced textured

superhydrophobic silver-perfluorodecanethiolate complexes on coated polystyrene (PS) surfaces. Modifying the ratio of $AgNO_3$ and perfluorodecanethiol changed the roughness of the surfaces produced. Subsequent UV irradiation led to silver nanoparticles formation on the surfaces. Upon soaking unmodified PS, non UV-treated surface (nonsuperhydrophobic), and UV-treated surface (superhydrophobic) for 9 hours in PAO1 containing bacterial broth, the PS surfaces exhibited significant bacterial binding and growth on the surface after exposure. The superhydrophobic surfaces without UV exposure showed some binding, but significantly less than non-superhydrophobic PS surfaces. The UV-treated superhydrophobic surfaces showed the least bacterial binding and growth. Shateri Khalil-Abad *et al.* [182] fabricated cotton textiles with silver nanoparticles by first treating with base followed by exposure to $AgNO_3$. Further modification with octyltriethoxysilane produced a superhydrophobic surface with dual-scale roughness. With the release of silver ions from the material, they showed activity against Gram-positive and Gram-negative bacteria. Spasova *et al.* [183] manufactured nanofiber meshes composed of poly(vinylidene fluoride) or poly(vinylidene fluoride-*co*-hexafluoropropylene) containing ZnO nanoparticles or the antibacterial drug 5-chloro-8-hydroxyquinolinol (5Cl8HQ). The ZnO-loaded meshes exhibited contact angles >150° and suppressed *S. aureus* growth over 24 hours compared to the unloaded meshes. Meshes loaded with 5Cl8HQ also afforded a zone of *S. aureus* and *E. coli* inhibition.

There are ongoing efforts to commercialize superhydrophobic coatings to reduce device-associated infections, but none are yet on the market. A Phase I SBIR granted to Taton *et al.* at Innovative Surface Technologies, LLC explored a superhydrophobic, chlorhexidine-releasing coating for endotracheal tubes to prevent ventilator-associated pneumonia [184]. The results are said to be promising, and the company is seeking a medical device partner for commercialization (personal communication with Dr. Taton). Another Phase I SBIR was granted to Lalwani *et al.* at Lynntech, Inc., towards developing superhydrophobic coatings for catheters to prevent urinary tract infection [185], and results will be forthcoming.

In contrast to the goals of preventing bacterial growth and adhesion, several reports describe superhydrophobic surfaces promoting bacteria growth. Dou *et al.* [186] recreated the topology of the rose petal using different polymer mixtures, and reported that the greatest adhesion of Gram-positive bacteria occurred at an intermediate hydrophobicity. Sousa *et al.* [187] showed that bacteria grew better on superhydrophobic PLLA substrates when incubated with *S. aureus* or *P. aeruginosa* for 24 hours compared to flat PLLA surfaces (2-log reduction). Fadeeva *et al.* [75] produced Lotus leaf mimics using titanium substrates and laser ablation that produced features of 10-20 μm with dual roughness features of about 200 nm. Non-laser ablated surfaces exhibited CA of 73°, where after laser treatment the apparent contact angles are as high as 166°. Increased colonization of *S. aureus* is observed on the superhydrophobic surfaces compared to the flat surfaces. *P. aeruginosa* colonization is slightly reduced on the textured titanium surface, which may be a result of the biophysical effects of rigid nano-scale pillars (independent of entrapped air) upon Gram-negative bacteria, discussed previously [174].

Superhydrophobic materials can suppress bacterial adsorption and growth on implants during the crucial perioperative time period. The maintenance of air reduces the area to bind.

Release of antibacterial agents from superhydrophobic materials further increases efficacy. This application is particularly promising because the air needs to be maintained on the material only temporarily.

7. Diagnostic Applications

Superhydrophobic surfaces are being explored for “Lab-on-a-Chip” diagnostics. Highlighted briefly in previous sections, superhydrophobic substrates can be patterned such that select regions remain superhydrophobic, and others modified to be hydrophobic, hydrophilic, or superhydrophilic. These patterning processes define regions with different wettability to favor selective deposition of molecules or cells or the movement of fluid from one area to another.

Superhydrophobic surfaces, for example, are used to stabilize droplets, drive flow, or act as valves in microfluidic diagnostics, as reviewed recently by Gogolides *et al.* [188]. For example, Li *et al.* [189] employed a PTFE powder cured by UV to create a superhydrophobic coating. When 10 μL droplets of blood are mixed with anti-A, -B or -D antibodies, added onto the surface, and imaged over 180 s, the high apparent contact angles of the blood droplets facilitated color differentiation from the haemagglutination reaction that corresponded to the blood type. Xin *et al.* [190] manufactured a surface with a less hydrophobic channel in a superhydrophobic PDMS surface using laser sintering. Droplets added to the one end of the channel flowed to specific regions due to the hydrophobicity differences. Elsharkawy *et al.* [191] prepared similar channels using an inkjet printer to cast a fluoropolymer on sandpaper. Lai *et al.* [192] manufactured a microchip using a vapor-diffusion self-assembled-monolayer method, where a superhydrophobic-tohydrophilic gradient was built into the chip to force migration of a water droplet across the surface. The wettability gradient controls the change in the velocity of the liquid flow, and the device can be fabricated so that droplet movement is bidirectional.

Surfaces with switchable wetting are also being investigated for diagnostics applications. Shiu *et al.* [193] demonstrated the ability to switch a surface from superhydrophobic to complete wetted with application of an applied electric field (electrowetting), allowing an array of protein microspots to selectively form. Before application of the electric field, protein binding is inhibited, allowing protein binding to be turned on or off. A widely investigated material for stimuli-responsive wetting is TiO_2, because under UV irradiation it exhibits photocatalysis and generates hydroxyl groups to make a rough surface superhydrophilic [35]. Meng *et al.* [194] employed surfaces with rough TiO_2 nanostructure to capture cells and adhere antibodies for diagnosis. The TiO_2 surfaces can be reused by photocatalytic cleaning under UV light to afford the original properties. The authors demonstrated four cycles of this process while maintaining the same cell capture efficiency and complete removal of protein as measured by immunofluorescence. Long-term maintenance of superhydrophobic materials may require this type of periodic cleaning cycle. Another diagnostic with responsive wetting is the pressure-deformable membrane reported by Seo *et al* [195]. The authors fabricated an elastic, 275 μm thick PDMS membrane textured with ~2 μm wide pillars, and demonstrated that the curvature created by applying vacuum altered the local contact angle. This process can then be used to drive droplet flow

and merging, as well as mixing of reagents (e.g., siRNA and synthetic delivery vectors) to prepare supramolecular structures for effective siRNA transfection.

Another elegant approach using superhydrophobic materials is to facilitate evaporative concentration of samples to small areas to aid detection. De Angelis *et al.* and Gentile *et al.* [196,197] used superhydrophobic surfaces for detecting extremely low concentrations of biomolecules. The authors fabricated a superhydrophobic surface of silicon micropillars and applied very dilute solutions of rhodamine, lambda DNA, or lysozyme in femto- to attomolar concentrations. When the solutions evaporate, the low concentrations of biomolecules selectively deposit on the pillars, with the protective air layer between pillars protecting other regions from deposition. Due to the low hysteresis, the droplets are not pinned during evaporation in this process, allowing the solute to be concentrated at a single, or several, pillar(s) (**Figure 8**). The specific nanofabrication technique used to produce their superhydrophobic surface allowed single molecule detection of the substances via an enhanced applied plasmonic field. Plasmonic techniques are sensitive to small concentrations, but sensing eventually becomes diffusion-limited. This technique overcomes these limitations, and the authors suggest its utility for detecting minute concentrations of cancer biomarkers. A similar approach is described by De Ninno et al. [198], where an array of Cr/Au nanorods are fabricated surrounded by a region of hydrophilic polymer, further surrounded by superhydrophobic PMMA pillars. This pattern confined the aqueous droplets to the region during evaporation, concentrating the protein on the nanorods for plasmonic detection. McLane *et al.* [199] used roll-to-roll manufacturing to emboss polyethylene with a high roughness and superhydrophobicity (CA of 154.6°). These materials served as a platform on which urine droplets from 2-20 μL with varying albumin levels are evaporated completely, and a colorimetric albumin assay on the dried sample spots afforded a 160-fold increase in sensitivity.

Differences in wetting can themselves be used as the output of a sensor, as in the selectively wetting mesh sensor we reported in Falde *et al.* [200]. Our approach used electrospun poly(ε-caprolactone) (PCL) based meshes with a top layer of controlled hydrophobicity that wets at a critical surface tension, after which a lower hydrophilic layer with a bromocresol purple dye causes a pH-dependent color change. Tuning the critical surface tension by changing the content of hydrophobic poly(glycerol monostearate-*co*-ε-caprolactone) (PGC-C18) enabled these meshes to act as surface tension sensors with a ≤2 mN/m resolution using the naked eye, enough to allow determination of clinically relevant changes in urine bile acid concentration or breast milk fat content. A more specific sensor application by Qing *et al.* [201] used 3-(acryloylthioureido) phenylboronic acid-copoly(N-isopropylacrylamide), (ATPBA)-*co*-pNIPAAm, which displayed saccharide-sensitive wettability, with a flat contact angle of 81° in pure water but 43° in a 0.05 M glucose solution. When this polymer is coated on an array of silicon pillars, the sensitivity is greatly increased, exhibiting apparent contact angles of 156° and 0° with the pure water and 0.05 M glucose solutions. A 10° change in response to a 0.1 mM glucose change is detected. Further work by Qing *et al.* described chirality-sensitive saccharide [202] and nucleotide-sensitive [203] versions of these sensors. These applications demonstrate that with appropriate

engineering of the superhydrophobic surface, detection of minute changes in the surface tension of liquids and solutions of important analytes is attainable.

Sensor applications at the cellular level employ superhydrophobic surfaces to enable the patterning of cells for high throughput diagnostic devices. Techniques for fabrication of these patterned surfaces are recently reviewed by Ueda and Levkin [204] and the reader is referred to this article. Neto *et al.* [205] designed a patterned superhydrophobic microarray for the high-throughput screening of the interactions between biomaterials, proteins, and cells. PS superhydrophobic surfaces are manufactured via a phase-separation technique. The wettability of different regions on the surface is tuned with varied UVO treatment. The ratio, amount, and adsorption time of human serum albumin and human plasma FN are varied to probe adsorption characteristics of regions with different wettabilities. These permutations are then used to study the cell adhesion of osteoblast-like cells, where different protein combinations and the hydrophilicity of the surfaces modulate cell binding. The authors suggest this surface can be used as a high throughput method to evaluate biomaterial surfaces and their protein and cell binding characteristics. Geyer *et al.* [206] produced an array of superhydrophilic spots separated by superhydrophobic barriers. Treating the HEMA-EDMA surfaces with UVO followed by grafting a fluorinated brush polymer afforded superhydrophobicity. When the surfaces are incubated with cells, only the superhydrophilic regions bind cells, and the superhydrophobic barrier regions showed less cell binding as a result of air trapped at the surface. This phenomenon is furthered examined by plating cells expressing mCherry or GFP in different regions to produce “wells” of varied cell types. Shiu *et al.* [207] manufactured cell microarrays by varying surface roughness and tuning wettability. Rougher surfaces hosted increased numbers of cells after 3 hours. Initially the rougher, more superhydrophobic surfaces resisted protein adsorption, but at later times lead to enhanced protein adsorption and cell growth.

Superhydrophobic materials provide useful platforms for supporting and handling microliter-scale droplets commonly used in many diagnostics, especially miniaturized point-of-care devices. The wetting transition from the Cassie-Baxter to Wenzel states serves either as an indicator itself or as a driver of flow for microfluidic assays. Alternatively, superhydrophobic surfaces stabilize small droplets for detection or to enhance evaporative concentration. Finally, superhydrophobic surfaces can drive cell patterning for microarray assays. These diagnostic applications are promising as the stability of the air layer at the superhydrophobic surface is only transiently required.

8. Drug delivery

Drug delivery is an exceedingly active research area with the primary goal of more effectively delivering a therapeutic agent to a target site. In cancer treatment, for example, the current standard of care often involves chemotherapeutics delivered as an intravenous bolus, leading to systemic drug distribution and only a small fraction of this drug reaching the target. This non-specific delivery leads to significant dose limiting side effects and overall poor clinical outcomes. Thus, a significant focus of the drug delivery community is the design and evaluation of delivery systems fabricated from polymers, lipids, and ceramics that encapsulate a therapeutic agent. This includes particle-based systems (nanoparticle,

micelles, liposomes, dendrimers, others), where the particle encapsulates the drug and improves targeting to a site, as well as drug depots (microparticles, microrods, films, meshes, others) which are designed to be implanted directly at the target site to release drug over a constant rate and a specified time [208–212]. Research on both particle- and depot-based drug delivery systems aim to improve treatment options by decreasing systemic toxicities, increasing bioavailability, and improving the solubility of the drug.

The Mano group used superhydrophobic surfaces to fabricated hydrogel beads containing drugs or cells. For example, small (5-10 μL) aqueous droplets of dextranmethacrylate and pNIPAAM mixed with model proteins insulin or albumin are confined on superhydrophobic surfaces for subsequent UV-curing [213]. The cross-linked particles exhibited temperature-responsive drug delivery over 48 hours. The same group also recently demonstrated a similar process using milder conditions suitable for encapsulating growth factors with living cells for skin repair [214]. Droplets of collagen mixed with platelet lysate and human adipose-derived stem cells are added to superhydrophobic surfaces and allowed to gel for 10-15 minutes. The beads released protein over about 8 hours, and cell growth continued for 7 days.

Metastable superhydrophobic materials are themselves being investigated as delivery platforms because the rate of wetting controls drug release from the material. In general, drug delivery from electrospun fibers is an active area of research and techniques for electrospinning nanofibers are reviewed by Hu *et al.* and Chou *et al.* [215,216]. Reports from our laboratory [76–78,217,218] describe the fabrication and characterization of superhydrophobic 3D materials as drug delivery devices. By varying the stability of an entrapped air layer within these 3D materials, the rate of drug release is controlled.

Superhydrophobic 3D materials are fabricated using electrospinning with blends of the biocompatible polymers PCL and PGC-C18 (poly(glycerol monostearate carbonate-*co*-caprolactone). PGC-C18 is significantly more hydrophobic than PCL (contact angle of 116° versus 83° for flat materials), and further additions of PGC-C18 into electrospun meshes afforded increased stability of the entrapped air layer. Increasing the hydrophobicity of the meshes lead to slower air removal when submerged in water, taking 10 to 75 days, or with sufficient superhydrophobicity, a permanently stable air layer [217]. When meshes are loaded with a camptothecin derivative SN-38, the rate of removal of the entrapped air layer within superhydrophobic meshes directly controls the drug release rate. Further, when the drug is loaded only in a central layer, the drug release is delayed until that layer is wetted (as verified with CT imaging), extending release to over 100 days in PBS, or 40 days in a mechanically agitated 10% serum solution [78], as shown in **Figure 9**, again reinforcing the effect of protein on the time scale of air maintenance. These drug-eluting superhydrophobic meshes are effective in *in vitro* cytotoxicity assay, killing a variety of cancer cell lines (lung, colon, breast) over 2 to >10 weeks [76,78]. Additionally, mechanical forces such as ultrasound (pressure) can be used to forcefully remove the air layer from the superhydrophobic material and trigger drug release [219]. One potential application for these devices is as a combination buttressing-drug delivery device for resectable lung cancer. However, this work also highlights the importance of release media and mechanical forces on the rate of wetting and drug release.

In a related study, Manna *et al.* [220] employed layer-by-layer assembly to fabricate superhydrophobic coatings ~80 μm thick using the polyelectrolytes poly(ethyleneimine) and poly(2-vinyl- 4,4-dimethylazlactone). These coatings, loaded with either a rhodamine dye or the anti-biofilm agent 2-aminobenzimidazole, afforded release of the loaded drug or drug model for ~300 days.

Further work by Kaplan *et al.* in the Grinstaff laboratory [221] investigated the release of cisplatin from electrospun superhydrophobic meshes, again using PCL and PGC-C18 polymer blends. Drug release and extended cytotoxicity against Lewis Lung Carcinoma (LLC) cells is observed over 90 days, which corresponded to the infiltration time for a solution of 10% fetal bovine serum (FBS), as imaged by CT. To our knowledge, this is the longest reported underwater layer maintenance in the presence of significant protein. These meshes, when implanted into mice in a subcutaneous LLC resection model, demonstrated increased prevention of local recurrence compared to systemic cisplatin as well as local biocompatibility. Finally, Wang and Kaplan, *et al.* explored the use of superhydrophobic, electrosprayed coatings as a mechano-responsive drug delivery system where release of either a hydrophilic or a hydrophobic drug is controlled by the amount of applied strain. In this system, the drug loaded core is sandwiched between two superhydrophobic, electrosprayed coatings, and the applied mechanical force induced cracks in the coating with subsequent release of the drugs [222].

Mesoporous silica nanoparticles are being explored for drug delivery, therapeutic ultrasound, and as ultrasound contrast agents. Zhao *et al.* synthesized nanoparticles with hydrophobic pores which, after cell internalization and application of low-energy ultrasound, resulted in cell death due to released nanobubbles [223]. These particles are even more effective if the pores have closed ends, suggesting that they entrap air in addition to serving as nucleation sites for cavitation. Ahmad Nor *et al.* prepared similar particles, with varying degrees of hydrophobicity, and demonstrated that the particles which were both rough and hydrophobic released their drug loadings slowest [224]. Yildrim *et al.* reported that mesoporous silica nanoparticles are effective ultrasound contrast agents, by releasing or nucleating microbubbles in response to focused ultrasound [225]. Finally, Chen *et al.* synthesized mesoporous silica nanoparticles with grafted fluorocarbons and photoresponsive spiropyran [226]. The authors showed UV-triggered release of loaded fluorescein disodium and camptothecin. This is a surprisingly dramatic change given that similar functionalization on silica pillars causes pinning but no noticeable change in the advancing contact angle.

Superhydrophobic materials present a promising new platform for drug delivery. With proper choice of materials, drugs, and method of drug loading, the release kinetics can be tuned for a variety of applications. Superhydrophobic materials are amenable to the delivery of both hydrophobic and hydrophilic agents. The time scales for delivery are controlled from a few days to the order of months, even in rigorous conditions, and superhydrophobic drug delivery devices, at least in one example, exhibit efficacy *in vivo*.

9. Conclusions, Perspectives, and Future Directions

Superhydrophobic materials exhibit a number of unique properties that arise from the high roughness of a low surface energy material that stabilizes a non-wetted state. A wide selection of materials and a number of top down and bottom up approaches are available for fabrication, including several that are practiced on the commercial scale such as precipitation, CVD, electrospinning, soft lithography, and embossing. The Wenzel and Cassie-Baxter models provide a mathematical description of the fully wetted and partially wetted states, and a means for predicting material wettability. Modeling studies have resulted in re-entrant topology designs that are remarkably superhydrophobic and even omniphobic [86,227–229]. However, modeling is more challenging with materials possessing variable topology such as electrospun meshes.

In biomedical applications, the wetted state is best viewed as metastable, where the maintenance of this state is highly dependent on the materials, morphology, initial wetting state, and solutes and surfactants in the liquid. Furthermore, the stability of this state is sensitive to its local conditions where a sufficient treatment with vibration, acoustic pressure, hydraulic pressure, or changes in surface energy (e.g., addition of a surfactant) will afford wetting and removal of the air layer. This is especially relevant for biomedical applications where salts, surfactants (e.g. albumin), and mechanical forces (tension and compression) are prevalent. This metastability is either an advantage or disadvantage, depending on the application.

The prevention of protein adsorption is a major focus is being investigated. In general, superhydrophobic surfaces possessing higher apparent contact angles prevent protein adsorption over longer time periods than those with lower contact angles. Several groups report selective protein adsorption based on the curvature of a structure alone, suggesting that any material may possess an anti-fouling feature. However, as these surfaces exhibit a large surface area, once wetted, the total protein adsorption is significantly greater than for the corresponding smooth, flat surfaces. Stimuli-responsive systems that refresh and clean a surface will likely extend the useful lifetime of these materials.

For many *in vitro* and *in vivo* applications, cellular attachment to a substrate is a prerequisite. The presence of entrapped air limits cells from interacting with the material surface. The roughness and curvature present on the superhydrophobic surface affect cell spreading and proliferation, with materials possessing greater contact angles reducing both cellular activities. Superhydrophobic-superhydrophilic patterned surfaces allow the precise seeding of different cell types in closely adjacent arrays, allowing co-culture of cells for use in diagnostics, cell signaling studies, and tissue engineering over a few days.

Similarly, bacterial adsorption and growth can be inhibited for over three days by reducing the wetted area available for bacterial adsorption. Antibacterial agents can be incorporated and released over time, either as a bolus or by slow elution during material wetting as in the drug delivery applications. Furthermore, there are examples showing that the rough morphology of a surface can itself inhibit the growth of Gram-negative bacteria through a biophysical effect. Since the reduction in bacterial adhesion and growth in the first hours and

days can significantly reduce overall infection rates, this is one of the most promising applications of superhydrophobic materials.

Superhydrophobic biomaterials are also being evaluated in more demanding biological applications, such as the prevention of blood coagulation. The demand for new blood-compatible materials is large given their use in vascular grafts to hemodialysis. Superhydrophobic surfaces exhibit reduced platelet attachment and coagulation with increased contact angle. Blood compatibility is observed only for relatively short periods of time (<2 hours) after which materials adsorb proteins and cells.

Additionally, superhydrophobic materials provide useful platforms for supporting and handling microliter-scale droplets in diagnostics. Patterns of hydrophilic and superhydrophobic areas facilitate droplet stabilization for high throughput assays or control liquid flow in microfluidics.

Tunable delivery of both hydrophobic and hydrophilic drugs is also demonstrated from superhydrophobic materials. The ability to control wetting is used to slow dissolution of drug entrapped in superhydrophobic meshes, coatings, or nanoparticles. Drug release is demonstrated for weeks under rigorous *in vitro* conditions, and efficacy is observed in an *in vivo* model of local cancer recurrence, though extending the non-wetted state remains a significant challenge.

The above observations and results suggest a number of additional basic research avenues, such as: 1) materials which can maintain the Cassie-Baxter state in protein solutions and *in vivo* for months as opposed to weeks; 2) refinement of the relationships between stability of the meta-stable state and acoustic pressure, hydraulic pressure, surfactant composition, or surfactant concentration; 3) identification of materials and processes suitable for delivery of proteins, as current reports are focused solely on small molecule delivery; and 4) further development of stimuli-responsive and reversibly wetting superhydrophobic/superhydrophilic materials.

To our knowledge there are no FDA-approved (or CE marked) medical devices that employ superhydrophobic surfaces, however, there is precedence for the commercialization of products exhibiting superhydrophobicity. This is especially evident in the self-cleaning and anti-icing areas. Multiple aerosol and liquid paints that are on the market produce superhydrophobic and self-cleaning coatings on a variety of substrates, including NeverWet from Rust-Oleum, Ultra-Ever Dry from UltraTech International, and WX2100 from Cytonix. The latter is typical of the group, a mixture of 25 μm and 200 nm silica particles in a fluorourethane liquid [230], which dries into a coating with dual-scale roughness and a static contact angle of 156° [231]. Fabric treatments are also being marketed as producing superhydrophobic materials, including EverShield from UltraTech. These commercial successes provide motivation for the translation of superhydrophobic biomaterials for use in clinical applications. Potential biomaterial product concepts, to name a few, include: 1) catheters, endotracheal tubes, or medical instruments with a superhydrophobic coating to reduce bacterial adhesion when in contact with blood or bodily fluids; 2) controlled patterns of superhydrophobic and superhydrophilic areas used to construct cellular microarrays or

engineered tissues; 3) disposable microfluidic diagnostic devices, , where the superhydrophobic coating supports droplets or facilitates fluid flow; and 4) coated medical devices for drug delivery such as a drug eluting lung tissue buttressing device.

The purpose of this manuscript is to review the state-of-the art in superhydrophobic biomaterials, to promote new research, and to stimulate discussion. We encourage all to investigate this exciting area of biomaterials and its potential clinical applications.

Supplementary Material

Refer to Web version on PubMed Central for supplementary material.

Acknowledgment

The authors thank BU, the National Institute of Health (R01CA149561 and R01EB017722), and National Science Foundation (DMR1507081) for support. M.W.G. also thanks his past and current students and postdoctoral fellows as well as our many clinical collaborators and colleagues for their hard work and dedication to synthesizing and evaluating new superhydrophobic biomaterials for drug delivery and diagnostic applications.

References

1. Marmur A. Superhydrophobic and superhygrophobic surfaces: from understanding non-wettability to design considerations. Soft Matter. 2013; 9:7900–7904.
2. Cassie ABD, Baxter S. Wettability of porous surfaces. Trans. Faraday Soc. 1944; 40:546–551.
3. Wenzel RN. Resistance of solid surfaces to wetting by water. J. Ind. Eng. Chem. 1936; 28:988–994.
4. Barthlott W, Neinhuis C. Purity of the sacred lotus, or escape from contamination in biological surfaces. Planta. 1997; 202:1–8.
5. Wagner P, Fürstner R, Barthlott W, Neinhuis C. Quantitative assessment to the structural basis of water repellency in natural and technical surfaces. J. Exp. Bot. 2003; 54:1295–1303. [PubMed: 12654881]
6. Bhushan B, Jung YC. Micro-and nanoscale characterization of hydrophobic and hydrophilic leaf surfaces. Nanotechnology. 2006; 17:2758.
7. Guo Z, Liu W. Biomimic from the superhydrophobic plant leaves in nature: Binary structure and unitary structure. Plant Sci. 2007; 172:1103–1112.
8. Koch K, Barthlott W. Superhydrophobic and superhydrophilic plant surfaces: an inspiration for biomimetic materials. Phil. Trans. R. Soc. A. 2009; 367:1487–509. [PubMed: 19324720]
9. Thorpe WH. Plastron respiration in aquatic insects. Biol. Rev. 1950; 25:344–390. [PubMed: 24538378]
10. Noble-Nesbitt J. Transpiration in Podura aquatica L.(Collembola, Isotomidae) and the wetting properties of its cuticle. J. Exp. Biol. 1963; 40:681–700.
11. Heckman CW. Comparative morphology of arthropod exterior surfaces with the capability of binding a film of air underwater. Int. Rev. Der Gesamten Hydrobiol. Und Hydrogr. 1983; 68:715–736.
12. Wagner T, Neinhuis C, Barthlott W. Wettability and contaminability of insect wings as a function of their surface sculptures. Acta Zool. 1996; 77:213–225.
13. Gao X, Jiang L. Biophysics: water-repellent legs of water striders. Nature. 2004; 432:36. [PubMed: 15525973]
14. Shirtcliffe NJ, McHale G, Newton MI, Perry CC, Pyatt FB. Plastron properties of a superhydrophobic surface. Appl. Phys. Lett. 2006; 89:104106/1–104106/2.
15. Bush JWM, Hu DL, Prakash M. The integument of water-walking arthropods: form and function. Adv. Insect Physiol. 2007; 34:117–192.

16. Gao X, Yan X, Yao X, Xu L, Zhang K, Zhang J, et al. The Dry-Style Antifogging Properties of Mosquito Compound Eyes and Artificial Analogues Prepared by Soft Lithography. Adv. Mater. 2007; 19:2213–2217.
17. Bormashenko E, Bormashenko Y, Stein T, Whyman G. Why do pigeon feathers repel water? Hydrophobicity of pennae, Cassie–Baxter wetting hypothesis and Cassie–Wenzel capillarity-induced wetting transition. J. Colloid Interface Sci. 2007; 311:212–216. [PubMed: 17359990]
18. Srinivasan S, Chhatre SS, Guardado JO, Park K-C, Parker AR, Rubner MF, et al. Quantification of feather structure, wettability and resistance to liquid penetration. J. R. Soc. Interface. 2014; 11:20140287. [PubMed: 24789563]
19. Cassie ABD, Baxter S. Large contact angles of plant and animal surfaces. Nature. 1945; 155:21–22.
20. Parker AR, Lawrence CR. Water capture by a desert beetle. Nature. 2001; 414:33–34. [PubMed: 11689930]
21. Webb HK, Crawford RJ, Ivanova EP. Wettability of natural superhydrophobic surfaces. Adv. Colloid Interface Sci. 2014; 210:58–64. [PubMed: 24556235]
22. Feng L, Li S, Li Y, Li H, Zhang L, Zhai J, et al. Super-hydrophobic surfaces: From natural to artificial. Adv. Mater. 2002; 14:1857–1860.
23. Nosonovsky M, Bhushan B. Superhydrophobic surfaces and emerging applications: Non-adhesion, energy, green engineering. Curr. Opin. Colloid Interface Sci. 2009; 14:270–280.
24. Guo Z, Liu W, Su BL. Superhydrophobic surfaces: From natural to biomimetic to functional. J. Colloid Interface Sci. 2011; 353:335–355. [PubMed: 20846662]
25. K Webb H, Hasan J, K Truong V, J Crawford R, P Ivanova E. Nature inspired structured surfaces for biomedical applications. Curr. Med. Chem. 2011; 18:3367–3375. [PubMed: 21728964]
26. Ma M, Mao Y, Gupta M, Gleason KK, Rutledge GC. Superhydrophobic fabrics produced by electrospinning and chemical vapor deposition. Macromolecules. 2005; 38:9742–9748.
27. Li X-M, Reinhoudt D, Crego-Calama M. What do we need for a superhydrophobic surface? A review on the recent progress in the preparation of superhydrophobic surfaces. Chem. Soc. Rev. 2007; 36:1350–1368. [PubMed: 17619692]
28. Ma M, Hill RM, Rutledge GC. A review of recent results on superhydrophobic materials based on micro- and nanofibers. J. Adhes. Sci. Technol. 2008; 22:1799–1817.
29. Roach P, Shirtcliffe NJ, Newton MI. Progress in superhydrophobic surface development. Soft Matter. 2008; 4:224–240.
30. Zhang X, Shi F, Niu J, Jiang Y, Wang Z. Superhydrophobic surfaces: from structural control to functional application. J. Mater. Chem. 2008; 18:621–633.
31. Xue CH, Jia ST, Zhang J, Ma JZ. Large-area fabrication of superhydrophobic surfaces for practical applications: an overview. Sci. Technol. Adv. Mater. 2010; 11:33002.
32. Yan YY, Gao N, Barthlott W. Mimicking natural superhydrophobic surfaces and grasping the wetting process: A review on recent progress in preparing superhydrophobic surfaces. Adv. Colloid Interface Sci. 2011; 169:80–105. [PubMed: 21974918]
33. Xue C-H, Ma J-Z. Long-lived superhydrophobic surfaces. J. Mater. Chem. A. 2013; 1:4146.
34. Celia E, Darmanin T, Taffin de Givenchy E, Amigoni S, Guittard F. Recent advances in designing superhydrophobic surfaces. J. Colloid Interface Sci. 2013; 402:1–18. [PubMed: 23647693]
35. Liu K, Cao M, Fujishima A, Jiang L. Bio-Inspired Titanium Dioxide Materials with Special Wettability and Their Applications. Chem. Rev. 2014; 114:10044–10094. [PubMed: 24956456]
36. Yao X, Song Y, Jiang L. Applications of Bio Inspired Special Wettable Surfaces. Adv. Mater. 2011; 23:719–734. [PubMed: 21287632]
37. Zhang D, Wang L, Qian H, Li X. Superhydrophobic surfaces for corrosion protection: a review of recent progresses and future directions. J. Coat. Technol. Res. 2015; 13:11–29.
38. Voronov RS, V Papavassiliou D, Lee LL. Review of fluid slip over superhydrophobic surfaces and its dependence on the contact angle. Ind. Eng. Chem. Res. 2008; 47:2455–2477.
39. Rothstein JP. Slip on superhydrophobic surfaces. Annu. Rev. Fluid Mech. 2010; 42:89–109.
40. Ferrari M, Benedetti A. Superhydrophobic surfaces for applications in seawater. Adv. Colloid Interface Sci. 2015; 222:291–304. [PubMed: 25759005]

41. Plawsky JL, Ojha M, Chatterjee A, Wayner PC Jr. Review of the effects of surface topography, surface chemistry, and fluid physics on evaporation at the contact line. Chem. Eng. Commun. 2008; 196:658–696.
42. Oberli L, Caruso D, Hall C, Fabretto M, Murphy PJ, Evans D. Condensation and freezing of droplets on superhydrophobic surfaces. Adv. Colloid Interface Sci. 2014; 210:47–57. [PubMed: 24200089]
43. Miljkovic N, Wang EN. Condensation Heat Transfer on Superhydrophobic Surfaces. MRS Bull. 2013; 38:397–406.
44. Verplanck N, Coffinier Y, Thomy V, Boukherroub R. Wettability switching techniques on superhydrophobic surfaces. Nanoscale Res. Lett. 2007; 2:577–596.
45. Heikenfeld J, Dhindsa M. Electrowetting on superhydrophobic surfaces: present status and prospects. J. Adhes. Sci. Technol. 2008; 3:319–334.
46. Xia F, Zhu Y, Feng L, Jiang L. Smart responsive surfaces switching reversibly between super-hydrophobicity and super-hydrophilicity. Soft Matter. 2009; 5:275–281.
47. Luong-Van E, Rodriguez I, Low HY, Elmouelhi N, Lowenhaupt B, Natarajan S, et al. Review: Micro- and nanostructured surface engineering for biomedical applications. J. Mater. Res. 2013; 28:165–174.
48. Lim JI, Il Kim S, Jung Y, Kim SH. Fabrication and medical applications of lotus-leaf-like structured superhydrophobic surfaces. Polymer (Korea). 2013; 37:411–419.
49. Darmanin T, Guittard F. Recent Advances in the Potential Applications of Bioinspired Superhydrophobic Materials. R. Soc. Chem. 2014; 2:16319–16359.
50. Lima AC, Mano JF. Micro/nano-structured superhydrophobic surfaces in the biomedical field: part II: applications overview. Nanomed. 2015; 10:271–97.
51. Lima AC, Mano JF. Micro/nano-structured superhydrophobic surfaces in the biomedical field: Part I: Basic concepts and biomimetic approaches. Nanomedicine (London, England). 2015; 10:103–19.
52. Shin S, Seo J, Han H, Kang S, Kim H, Lee T. Bio-inspired extreme wetting surfaces for biomedical applications. Materials. 2016; 9
53. Johnson RE, Dettre RH. Contact angle hysteresis, Contact Angle, Wettability. Adhes. Adv. Chem. Ser. 1964; 43:112–135.
54. Gao L, McCarthy TJ. Contact angle hysteresis explained. Langmuir. 2006; 22:6234–6237. [PubMed: 16800680]
55. Moraila-Martínez CL, Montes Ruiz-Cabello FJ, Cabrerizo-Vílchez MA, Rodríguez-Valverde MA. The effect of contact line dynamics and drop formation on measured values of receding contact angle at very low capillary numbers. Colloids Surfaces A Physicochem. Eng. Asp. 2012; 404:63–69.
56. Dettre RH, Johnson RE. Contact angle hysteresis II. Contact angle measurements on rough surfaces, Contact Angle, Wettability. Adhes. Adv. Chem. Ser. 1964; 43:136–144.
57. Cazabat AM, Stuart MAC. Dynamics of wetting: effects of surface roughness. J. Phys. Chem. 1986; 90:5845–5849.
58. Borgs C, De Coninck J, Kotecký R, Zinque M. Does the roughness of the substrate enhance wetting? Phys. Rev. Lett. 1995; 74:2292–2294. [PubMed: 10057891]
59. Rye RR, Mann Jr JA, Yost FG. The flow of liquids in surface grooves. Langmuir. 1996; 12:555–565.
60. Apel-Paz M, Marmur A. Spreading of liquids on rough surfaces. Colloids Surfaces A Physicochem. Eng. Asp. 1999; 146:273–279.
61. Bico J, Tordeux C, Quéré D. Rough wetting. Europhys. Lett. 2001; 55:214.
62. Jopp J, Grüll H, Yerushalmi-Rozen R. Wetting behavior of water droplets on hydrophobic microtextures of comparable size. Langmuir. 2004; 20:10015–10019. [PubMed: 15518488]
63. McHale G, Shirtcliffe NJ, Newton MI. Contact-angle hysteresis on super-hydrophobic surfaces. Langmuir. 2004; 20:10146–10149. [PubMed: 15518506]
64. Lafuma A, Quéré D. Superhydrophobic states. Nat. Mater. 2003; 2:457–460. [PubMed: 12819775]

65. Patankar NA. On the modeling of hydrophobic contact angles on rough surfaces. Langmuir. 2003; 19:1249–1253.
66. Marmur A. The lotus effect: superhydrophobicity and metastability. Langmuir. 2004; 20:3517–3519. [PubMed: 15875376]
67. Gao L, McCarthy TJ. Reply to “Comment on How Wenzel and Cassie Were Wrong by Gao and McCarthy,”. Langmuir. 2007; 23:13243.
68. Tuteja A, Choi W, Ma M, Mabry JM, Mazzella SA, Rutledge GC, et al. Designing Superoleophobic Surfaces. Science. 2007; 318:1618–1622. [PubMed: 18063796]
69. Wang S, Jiang L. Definition of superhydrophobic states. Adv. Mater. 2007; 19:3423–3424.
70. Swain PS, Lipowsky R. Contact angles on heterogeneous surfaces: A new look at Cassie's and Wenzel's laws. Langmuir. 1998; 14:6772–6780.
71. Wolansky G, Marmur A. The actual contact angle on a heterogeneous rough surface in three dimensions. Langmuir. 1998; 14:5292–5297.
72. Wolansky G, Marmur A. Apparent contact angles on rough surfaces: the Wenzel equation revisited. Colloids Surfaces A Physicochem. Eng. Asp. 1999; 156:381–388.
73. Patankar NA. Transition between Superhydrophobic States on Rough Surfaces. Langmuir. 2004; 20:7097–7102. [PubMed: 15301493]
74. Poetes R, Holtzmann K, Franze K, Steiner U. Metastable underwater superhydrophobicity. Phys. Rev. Lett. 2010; 105:166104/1–166104/4. [PubMed: 21230986]
75. Fadeeva E, Truong VK, Stiesch M, Chichkov BN, Crawford RJ, Wang J, et al. Bacterial retention on superhydrophobic titanium surfaces fabricated by femtosecond laser ablation. Langmuir. 2011; 27
76. Yohe ST, Herrera VLM, Colson YL, Grinstaff MW. 3D Superhydrophobic Electrospun Meshes as Reinforcement Materials for Sustained Local Drug Delivery Against Colorectal Cancer Cells. J. Control. Release. 2012; 162:92–101. [PubMed: 22684120]
77. Yohe ST, Colson YL, Grinstaff MW. Superhydrophobic materials for tunable drug release: Using displacement of air to control delivery rates. J. Am. Chem. Soc. 2012; 134:2016–2019. [PubMed: 22279966]
78. Falde EJ, Freedman JD, Herrera VLM, Yohe ST, Colson YL, Grinstaff MW. Layered superhydrophobic meshes for controlled drug release. J. Control. Release. 2015; 214:23–29. [PubMed: 26160309]
79. Ou J, Rothstein JP. Direct velocity measurements of the flow past drag-reducing ultrahydrophobic surfaces. Phys. Fluids. 2005; 17:103606/1–103606/10.
80. Truesdell R, Mammoli A, Vorobieff P, Van Swol F, Brinker CJ. Drag reduction on a patterned superhydrophobic surface. Phys. Rev. Lett. 2006; 97:044504/1–044504/4. [PubMed: 16907578]
81. McHale G, Newton MI, Shirtcliffe NJ. Immersed superhydrophobic surfaces: Gas exchange, slip and drag reduction properties. Soft Matter. 2010; 6:714–719.
82. Lee C, Kim CJ. Underwater restoration and retention of gases on superhydrophobic surfaces for drag reduction. Phys. Rev. Lett. 2011; 106:14502.
83. Fukagata K, Kasagi N, Koumoutsakos P. A theoretical prediction of friction drag reduction in turbulent flow by superhydrophobic surfaces. Phys. Fluids. 2006; 18:089901/1.
84. Marmur A. Super-hydrophobicity fundamentals: implications to biofouling prevention. Biofouling. 2006; 22:107–115. [PubMed: 16581675]
85. Bobji MS, Kumar SV, Asthana A, Govardhan RN. Underwater sustainability of the “Cassie” state of wetting. Langmuir. 2009; 25:12120–12126. [PubMed: 19821621]
86. Sarkar A, Kietzig A-M. Design of a robust superhydrophobic surface: thermodynamic and kinetic analysis. Soft Matter. 2015; 11:3733–3733. [PubMed: 25868457]
87. Bormashenko EA, Bormashenko Y. Wetting of Composite Surfaces: When and Why Is the Area Far from The Triple Line Important? J. Phys. Chem. C. 2013; 117:19552–19557.
88. “Leo” Liu T, Kim C-J. Turning a surface superrepellent even to completely wetting liquids. Science. 2014; 346:1096–1100. [PubMed: 25430765]

89. Bartolo D, Bouamrirene F, Verneuil E, Buguin A, Silberzan P, Moulinet S. Bouncing or sticky droplets: impalement transitions on superhydrophobic micropatterned surfaces. EPL (Europhysics Lett. 2006; 74:299.

90. Reyssat M, Pépin A, Marty F, Chen Y, Quéré D. Bouncing transitions on microtextured materials. Europhys. Lett. 2006; 74:306.

91. Sbragaglia M, Peters AM, Pirat C, Borkent BM, Lammertink RGH, Wessling M, et al. Spontaneous breakdown of superhydrophobicity. Phys. Rev. Lett. 2007; 99:156001. [PubMed: 17995188]

92. Sheng X, Zhang J. Air layer on superhydrophobic surface underwater. Colloids Surfaces A Physicochem. Eng. Asp. 2011; 377:374–378.

93. Mohammadi R, Wassink J, Amirfazli A. Effect of surfactants on wetting of super-hydrophobic surfaces. Langmuir. 2004; 20:9657–9662. [PubMed: 15491199]

94. Ferrari M, Ravera F, Rao S, Liggieri L. Surfactant adsorption at superhydrophobic surfaces. Appl. Phys. Lett. 2006; 89:053104/1–053104/3.

95. Chang F-M, Sheng Y-J, Chen H, Tsao H-K. From superhydrophobic to superhydrophilic surfaces tuned by surfactant solutions. Appl. Phys. Lett. 2007; 91:094108/1–094108/3.

96. Extrand CW. Designing for Optimum Liquid Repellency. Langmuir. 2006; 22:1711–1714. [PubMed: 16460095]

97. Gao L, McCarthy TJ. A Perfectly Hydrophobic Surface (θA/θR= 180°/180°). J. Am. Chem. Soc. 2006; 128:9052–9053. [PubMed: 16834376]

98. Horbett TA. Protein adsorption on biomaterials. Biomater. Interfacial Phenom. Appl. 1982; 199:233–244.

99. Young BR, Pitt WG, Cooper SL. Protein adsorption on polymeric biomaterials:: II. Adsorption kinetics. J. Colloid Interface Sci. 1988; 124:28–43.

100. Ratner BD, Hoffman AS. Nonfouling Surfaces. Biomater. Sci. an Introd. to Mater. Med. 2004:197–201.

101. Gombotz WR, Guanghui W, Horbett TA, Hoffman AS. Protein adsorption to poly (ethylene oxide) surfaces. J. Biomed. Mater. Res. 1991; 25:1547–1562. [PubMed: 1839026]

102. Antonsen KP, Hoffman AS. Water structure of PEG solutions by differential scanning calorimetry measurements. Top. Appl. Chem. Poly (Ethylene Glycol) Chem. Biotech. Biomed. Appl. 1992:15–28.

103. Lim K, Herron JN. Molecular simulation of protein-PEG interaction. Poly (Ethylene Glycol) Chem. Biotech. Biomed. Appl. 1992:29–56.

104. Prime KL, Whitesides GM. Adsorption of proteins onto surfaces containing end-attached oligo (ethylene oxide): a model system using self-assembled monolayers. J. Am. Chem. Soc. 1993; 115:10714–10721.

105. Harder P, Grunze M, Dahint R, Whitesides GM, Laibinis PE. Molecular conformation in oligo (ethylene glycol)-terminated self-assembled monolayers on gold and silver surfaces determines their ability to resist protein adsorption. J. Phys. Chem. B. 1998; 102:426–436.

106. Feldman K, Hähner G, Spencer ND, Harder P, Grunze M. Probing resistance to protein adsorption of oligo (ethylene glycol)-terminated self-assembled monolayers by scanning force microscopy. J. Am. Chem. Soc. 1999; 121:10134–10141.

107. Horbett TA, Hoffman AS. Bovine plasma protein adsorption onto radiation-grafted hydrogels based on hydroxyethyl methacrylate and N-vinyl-pyrrolidone. Amererican Chem. Soc. Adv. Chem. 1975; 145:254.

108. Löpez GP, Ratner BD, Tidwell CD, Haycox CL, Rapoza RJ, Horbett TA. Glow discharge plasma deposition of tetraethylene glycol dimethyl ether for fouling-resistant biomaterial surfaces. J. Biomed. Mater. Res. 1992; 26:415–439. [PubMed: 1601898]

109. Sheu MS, Hoffman AS, Terlingen JGA, Feijen J. A new gas discharge process for preparation of non-fouling surfaces on biomaterials. Clin. Mater. 1993; 13:41–45.

110. Lasic DD, Needham D. The “stealth” liposome: a prototypical biomaterial. Chem. Rev. 1995; 95:2601–2628.

111. Chapman RG, Ostuni E, Takayama S, Holmlin RE, Yan L, Whitesides GM. Surveying for surfaces that resist the adsorption of proteins. Screening. 2000; 11:13.
112. Luk YY, Kato M, Mrksich M. Self-assembled monolayers of alkanethiolates presenting mannitol groups are inert to protein adsorption and cell attachment. Langmuir. 2000; 16:9604–9608.
113. Ostuni E, Chapman RG, Holmlin RE, Takayama S, Whitesides GM. A survey of structure-property relationships of surfaces that resist the adsorption of protein. Langmuir. 2001; 17:5605–5620.
114. Shin H, Jo S, Mikos AG. Biomimetic materials for tissue engineering. Biomaterials. 2003; 24:4353–4364. [PubMed: 12922148]
115. Ratner BD, Bryant SJ. Biomaterials: Where we have been and where we are going. Annu. Rev. Biomed. Eng. 2004; 6:41–75. [PubMed: 15255762]
116. Latour RA. Biomaterials: Protein-surface interactions. Encycl. Biomater. Biomed. Eng. 2005; 1:270–278.
117. Goldberg M, Langer R, Jia X. Nanostructured materials for applications in drug delivery and tissue engineering. J. Biomater. Sci. Polym. Ed. 2007; 18:241. [PubMed: 17471764]
118. Meyers SR, Grinstaff MW. Biocompatible and bioactive surface modifications for prolonged in vivo efficacy. Chem. Rev. 2012; 112:1615–1632. [PubMed: 22007787]
119. Rechendorff K, Hovgaard MB, Foss M, Zhdanov VP, Besenbacher F. Enhancement of protein adsorption induced by surface roughness. Langmuir. 2006; 22:10885–10888. [PubMed: 17154557]
120. Roach P, Farrar D, Perry CC. Surface tailoring for controlled protein adsorption: effect of topography at the nanometer scale and chemistry. J. Am. Chem. Soc. 2006; 128:3939–3945. [PubMed: 16551101]
121. Mandal HS, Kraatz HB. Effect of the surface curvature on the secondary structure of peptides adsorbed on nanoparticles. J. Am. Chem. Soc. 2007; 129:6356–6357. [PubMed: 17458962]
122. Dolatshahi-Pirouz A, Rechendorff K, Hovgaard MB, Foss M, Chevallier J, Besenbacher F. Bovine serum albumin adsorption on nano-rough platinum surfaces studied by QCM-D. Colloids Surfaces B Biointerfaces. 2008; 66:53–59. [PubMed: 18586468]
123. Koc Y, De Mello AJ, McHale G, Newton MI, Roach P, Shirtcliffe NJ. Nano-scale superhydrophobicity: suppression of protein adsorption and promotion of flow-induced detachment. Lab Chip. 2008; 8:582–586. [PubMed: 18369513]
124. Shen L, Zhu J. Heterogeneous surfaces to repel proteins. Adv. Colloid Interface Sci. 2016; 228:40–54. [PubMed: 26691416]
125. Vogler EA. Protein adsorption in three dimensions. Biomaterials. 2011
126. Genzer J, Efimenko K. Recent developments in superhydrophobic surfaces and their relevance to marine fouling: a review. Biofouling. 2006; 22:339–360. [PubMed: 17110357]
127. Bixler GD, Bhushan B. Biofouling: lessons from nature. Philos. Trans. R. Soc. A Math. Phys. Eng. Sci. 2012; 370:2381–2417.
128. Leibner ES, Barnthip N, Chen W, Baumrucker CR, V Badding J, Pishko M, et al. Superhydrophobic effect on the adsorption of human serum albumin. Acta Biomater. 2009; 5:1389–1398. [PubMed: 19135420]
129. Huang Q, Lin L, Yang Y, Hu R, Vogler EA, Lin C. Role of trapped air in the formation of cell-and-protein micropatterns on superhydrophobic/superhydrophilic microtemplated surfaces. Biomaterials. 2012; 33:8213–8220. [PubMed: 22917736]
130. Accardo A, Gentile F, Mecarini F, De Angelis F, Burghammer M, Di Fabrizio E, et al. In situ X-ray scattering studies of protein solution droplets drying on micro-and nanopatterned superhydrophobic PMMA surfaces. Langmuir. 2010; 26:15057–15064. [PubMed: 20804171]
131. Choi C-H, Kim C-J. Droplet evaporation of pure water and protein solution on nanostructured superhydrophobic surfaces of varying heights. Langmuir. 2009; 25:7561–7567. [PubMed: 19518098]
132. Roach P, Shirtcliffe NJ, Farrar D, Perry CC. Quantification of surface-bound proteins by fluorometric assay: comparison with quartz crystal microbalance and amido black assay. J. Phys. Chem. B. 2006; 110:20572–20579. [PubMed: 17034246]

133. Zhai L, Berg MC, Cebeci FÇ, Kim Y, Milwid JM, Rubner MF, et al. Patterned superhydrophobic surfaces: Toward a synthetic mimic of the Namib Desert beetle. Nano Lett. 2006; 6:1213–1217. [PubMed: 16771582]

134. Lord MS, Foss M, Besenbacher F. Influence of nanoscale surface topography on protein adsorption and cellular response. Nano Today. 2010; 5:66–78.

135. Kurylowicz M, Paulin H, Mogyoros J, Giuliani M, Dutcher JR. The effect of nanoscale surface curvature on the oligomerization of surface-bound proteins. J. R. Soc. Interface / R. Soc. 2014; 11:20130818.

136. Ballester-Beltrán J, Rico P, Moratal D, Song W, Mano JF, Salmerón-Sánchez M. Role of superhydrophobicity in the biological activity of fibronectin at the cell–material interface. Soft Matter. 2011; 7:10803–10811.

137. Alves NM, Shi J, Oramas E, Santos JL, Tomás H, Mano JF. Bioinspired superhydrophobic poly (L lactic acid) surfaces control bone marrow derived cells adhesion and proliferation. J. Biomed. Mater. Res. Part A. 2009; 91:480–488.

138. Wang Y, Sims CE, Marc P, Bachman M, Li GP, Allbritton NL. Micropatterning of living cells on a heterogeneously wetted surface. Langmuir. 2006; 22:8257–8262. [PubMed: 16952271]

139. Di Mundo R, Nardulli M, Milella A, Favia P, D'Agostino R, Gristina R. Cell adhesion on nanotextured slippery superhydrophobic substrates. Langmuir. 2011; 27:4914–4921. [PubMed: 21413742]

140. Ranella A, Barberoglou M, Bakogianni S, Fotakis C, Stratakis E. Tuning cell adhesion by controlling the roughness and wettability of 3D micro/nano silicon structures. Acta Biomater. 2010; 6:2711–2720. [PubMed: 20080216]

141. Bauer S, Park J, Mark K, Schmuki P. Improved attachment of mesenchymal stem cells on super-hydrophobic TiO2 nanotubes. Acta Biomater. 2008; 4:1576–1582. [PubMed: 18485845]

142. Dowling DP, Miller IS, Ardhaoui M, Gallagher WM. Effect of surface wettability and topography on the adhesion of osteosarcoma cells on plasma-modified polystyrene. J. Biomater. Appl. 2011; 26:327–347. [PubMed: 20566655]

143. Oliveira SM, Song W, Alves NM, Mano JF. Chemical modification of bioinspired superhydrophobic polystyrene surfaces to control cell attachment/proliferation. Soft Matter. 2011; 7:8932–8941.

144. Ishizaki T, Saito N, Takai O. Correlation of cell adhesive behaviors on superhydrophobic, superhydrophilic, and micropatterned superhydrophobic/superhydrophilic surfaces to their surface chemistry. Langmuir. 2010; 26:8147–8154. [PubMed: 20131757]

145. Piret G, Galopin E, Coffinier Y, Boukherroub R, Legrand D, Slomianny C. Culture of mammalian cells on patterned superhydrophilic/superhydrophobic silicon nanowire arrays. Soft Matter. 2011; 7:8642–8649.

146. Efremov AN, Stanganello E, Welle A, Scholpp S, Levkin PA. Micropatterned superhydrophobic structures for the simultaneous culture of multiple cell types and the study of cell-cell communication. Biomaterials. 2013; 34:1757–1763. [PubMed: 23228425]

147. Popova AA, Demir K, Hartanto TG, Schmitt E, Levkin PA. Droplet-Microarray on Superhydrophobic-Superhydrophilic Patterns for High-Throughput Live Cell Screenings. RSC Adv. 2016; 6:38263–38276.

148. Neto AI, Correia CR, Oliveira MB, Rial-Hermida MI, Alvarez-Lorenzo C, Reis RL, et al. A novel hanging spherical drop system for the generation of cellular spheroids and high throughput combinatorial drug screening. Biomater. Sci. 2015; 3:581–5. [PubMed: 26222417]

149. Senesi GS, D'Aloia E, Gristina R, Favia P, d'Agostino R. Surface characterization of plasma deposited nano-structured fluorocarbon coatings for promoting in vitro cell growth. Surf. Sci. 2007; 601:1019–1025.

150. Gristina R, D'Aloia E, Senesi GS, Milella A, Nardulli M, Sardella E, et al. Increasing cell adhesion on plasma deposited fluorocarbon coatings by changing the surface topography. J. Biomed. Mater. Res. Part B Appl. Biomater. 2009; 88:139–149. [PubMed: 18618484]

151. Luo SC, Liour SS, Yu H. Perfluorofunctionalized PEDOT films with controlled morphology as superhydrophobic coatings and biointerfaces with enhanced cell adhesion. Chem. Commun. 2010; 46:4731–4733.

152. Desai M, Seifalian AM, Hamilton G. Role of prosthetic conduits in coronary artery bypass grafting. Eur. J. Cardiothorac. Surg. 2011; 40:394–398. [PubMed: 21216613]
153. Goodney PP, Beck AW, Nagle J, Welch HG, Zwolak RM. National trends in lower extremity bypass surgery, endovascular interventions, and major amputations. J. Vasc. Surg. 2009; 50:54–60. [PubMed: 19481407]
154. Akoh JA. Prosthetic arteriovenous grafts for hemodialysis. J. Vasc. Access. 2009; 10:137–147. [PubMed: 19670164]
155. Toes GJ, Van Muiswinkel KW, Van Oeveren W, Suurmeijer AJH, Timens W, Stokroos I, et al. Superhydrophobic modification fails to improve the performance of small diameter expanded polytetrafluoroethylene vascular grafts. Biomaterials. 2002; 23:255–262. [PubMed: 11763862]
156. Busscher HJ, Stokroos I, Golverdingen JG, Schakenraad JM. Adhesion and spreading of human fibroblasts on superhydrophobic FEP-Teflon. Cells Mater. 1991; 1:243–249.
157. Hou X, Wang X, Zhu Q, Bao J, Mao C, Jiang L, et al. Preparation of polypropylene superhydrophobic surface and its blood compatibility. Colloids Surfaces B Biointerfaces. 2010; 80:247–250. [PubMed: 20630719]
158. Sun T, Tan H, Han D, Fu Q, Jiang L. No platelet can adhere—largely improved blood compatibility on nanostructured superhydrophobic surfaces. Small. 2005; 1:959–963. [PubMed: 17193377]
159. Zhou M, Yang JH, Ye X, Zheng AR, Li G, Yang PF, et al. Blood Platelet's Behavior on Nanostructured Superhydrophobic Surface. J. Nano Res. 2008; 2:129–136.
160. Huang Q, Yang Y, Hu R, Lin C, Sun L, Vogler EA. Reduced platelet adhesion and improved corrosion resistance of superhydrophobic TiO2-nanotube-coated 316L stainless steel. Colloids Surfaces B Biointerfaces. 2015; 125:134–141. [PubMed: 25481855]
161. Nokes JM, Liedert R, Kim MY, Siddiqui A, Chu M, Lee EK, et al. Reduced Blood Coagulation on Roll-to-Roll. Shrink-Induced Superhydrophobic Plastics. 2016:1–9.
162. Darouiche RO. Treatment of infections associated with surgical implants. N. Engl. J. Med. 2004; 350:1422–1429. [PubMed: 15070792]
163. Hetrick EM, Schoenfisch MH. Reducing implant-related infections: active release strategies. Chem. Soc. Rev. 2006; 35:780–789. [PubMed: 16936926]
164. An YH, Friedman RJ. Prevention of sepsis in total joint arthroplasty. J. Hosp. Infect. 1996; 33:93–108. [PubMed: 8808743]
165. Nablo BJ, Rothrock AR, Schoenfisch MH. Nitric oxide-releasing sol–gels as antibacterial coatings for orthopedic implants. Biomaterials. 2005; 26:917–924. [PubMed: 15353203]
166. Poelstra KA, Barekzi NA, Rediske AM, Felts AG, Slunt JB, Grainger DW. Prophylactic treatment of gram-positive and gram-negative abdominal implant infections using locally delivered polyclonal antibodies. J. Biomed. Mater. Res. 2002; 60:206–215. [PubMed: 11835177]
167. Zhang X, Wang L, Levänen E. Superhydrophobic surfaces for reduction of bacterial adhesion. RCS Adv. 2013; 3:12003–12020.
168. Crick CR, Ismail S, Pratten J, Parkin IP. An investigation into bacterial attachment to an elastomeric superhydrophobic surface prepared via aerosol assisted deposition. Thin Solid Films. 2011; 519:3722–3727.
169. Tang P, Zhang W, Wang Y, Zhang B, Wang H, Lin C, et al. Effect of superhydrophobic surface of titanium on staphylococcus aureus adhesion. J. Nanomater. 2011; 2011:2–10.
170. Loo CY, Young P, Lee WH, Cavaliere R, Whitchurch CB, Rohanizadeh R. Superhydrophobic, nanotextured polyvinyl chloride films for delaying Pseudomonas aeruginosa attachment to intubation tubes and medical plastics. Acta Biomater. 2012; 8:1881–1890. [PubMed: 22330278]
171. Ma J, Sun Y, Gleichauf K, Lou J, Li Q. Nanostructure on taro leaves resists fouling by colloids and bacteria under submerged conditions. Langmuir. 2011; 27:10035–10040. [PubMed: 21736298]
172. Pernites RB, Santos CM, Maldonado M, Ponnapati RR, Rodrigues DF, Advincula RC. Tunable Protein and Bacterial Cell Adsorption on Colloidally Templated Superhydrophobic Polythiophene Films. Chem. Mater. 2012; 24:870–880.

173. Hasan J, Webb HK, Truong VK, Pogodin S, Baulin VA, Watson GS, et al. Selective bactericidal activity of nanopatterned superhydrophobic cicada Psaltoda claripennis wing surfaces. Appl. Microbiol. Biotechnol. 2013; 97:9257–9262. [PubMed: 23250225]
174. Pogodin S, Hasan J, Baulin VA, Webb HK, Truong VK, Phong Nguyen TH, et al. Biophysical model of bacterial cell interactions with nanopatterned cicada wing surfaces. Biophys. J. 2013; 104:835–840. [PubMed: 23442962]
175. Ivanova EP, Hasan J, Webb HK, Gervinskas G, Juodkazis S, Truong VK, et al. Bactericidal activity of black silicon. Nat. Commun. 2013; 4:2838. [PubMed: 24281410]
176. Hasan J, Raj S, Yadav L, Chatterjee K. Engineering a nanostructured “super surface” with superhydrophobic and superkilling properties. RSC Adv. 2015; 5:44953–44959.
177. Singh AV, Vyas V, Patil R, Sharma V, Scopelliti PE, Bongiorno G, et al. Quantitative characterization of the influence of the nanoscale morphology of nanostructured surfaces on bacterial adhesion and biofilm formation. PLoS One. 2011; 6:e25029. [PubMed: 21966403]
178. Hsu LC, Fang J, Borca-Tasciuc DA, Worobo RW, Moraru CI. Effect of micro- and nanoscale topography on the adhesion of bacterial cells to solid surfaces. Appl. Environ. Microbiol. 2013; 79:2703–2712. [PubMed: 23416997]
179. Berendjchi A, Khajavi R, Yazdanshenas ME. Fabrication of superhydrophobic and antibacterial surface on cotton fabric by doped silica-based sols with nanoparticles of copper. Nanoscale Res. Lett. 2011; 6:1–8.
180. Xue CH, Chen J, Yin W, Jia ST, Ma JZ. Superhydrophobic conductive textiles with antibacterial property by coating fibers with silver nanoparticles. Appl. Surf. Sci. 2011; 258:2468–2472.
181. Chung JS, Kim BG, Shim S, Kim SE, Sohn EH, Yoon J, et al. Silver-perfluorodecanethiolate Complexes Having Superhydrophobic, Antifouling, Antibacterial Properties. J. Colloid Interface Sci. 2012; 366:64–69. [PubMed: 22018531]
182. Shateri Khalil-Abad M, Yazdanshenas ME. Superhydrophobic antibacterial cotton textiles. J. Colloid Interface Sci. 2010; 351:293–298. [PubMed: 20709327]
183. Spasova M, Manolova N, Markova N, Rashkov I. Superhydrophobic PVDF and PVDF-HFP nanofibrous mats with antibacterial and anti-biofouling properties. Appl. Surf. Sci. 2016; 363:363–371.
184. Taton K. SBIR Phase I: Chlorhexidine Releasing Superhydrophobic Coatings. 2008
185. Lalwani, S. SBIR Phase I: Delayed Onset of Biofilm Formation and CAUTI with Superhydrophobic Catheters. 2011.
186. Dou XQ, Zhang D, Feng C, Jiang L. Bioinspired Hierarchical Surface Structures with Tunable Wettability for Regulating Bacteria Adhesion. ACS Nano. 2015; 9:10664–10672. [PubMed: 26434605]
187. Sousa C, Rodrigues D, Oliveira R, Song W, Mano JF, Azeredo J. Superhydrophobic poly (L-lactic acid) surface as potential bacterial colonization substrate. AMB Express. 2011; 1:34. [PubMed: 22018163]
188. Gogolides E, Ellinas K, Tserepi A. Hierarchical micro and nano structured, hydrophilic, superhydrophobic and superoleophobic surfaces incorporated in microfluidics, microarrays and lab on chip microsystems. Microelectron. Eng. 2015; 132:135–155.
189. Li L, Tian J, Li M, Shen W. Superhydrophobic surface supported bioassay - An application in blood typing. Colloids Surfaces B Biointerfaces. 2013; 106:176–180. [PubMed: 23434709]
190. Xing S, Harake RS, Pan T. Droplet-driven transports on superhydrophobic-patterned surface microfluidic. Lab Chip. 2011; 11:3642–3648. [PubMed: 21918770]
191. Elsharkawy M, Schutzius TM, Megaridis CM. Inkjet patterned superhydrophobic paper for open-air surface microfluidic devices. Lab Chip. 2014; 14:1168–75. [PubMed: 24481036]
192. Lai YH, Yang JT, Shieh DB. A microchip fabricated with a vapor-diffusion self-assembled-monolayer method to transport droplets across superhydrophobic to hydrophilic surfaces. Lab Chip. 2010; 10:499–504. [PubMed: 20126691]
193. Shiu JY, Chen PL. Addressable protein patterning via switchable superhydrophobic microarrays. Adv. Funct. Mater. 2007; 17:2680–2686.

194. Meng J, Zhang P, Zhang F, Liu H, Fan J, Liu X, et al. A Self-Cleaning TiO2 Nanosisal-like Coating toward Disposing Nanobiochips of Cancer Detection. ACS Nano. 2015; 9:9284–9291. [PubMed: 26285086]

195. Seo J, Lee SK, Lee J, Lee JS, Kwon H, Cho SW, et al. Path-programmable water droplet manipulations on an adhesion controlled superhydrophobic surface. Sci. Reports. 2015; 5:10.

196. De Angelis F, Gentile F, Mecarini F, Das G, Moretti M, Candeloro P, et al. Breaking the diffusion limit with super-hydrophobic delivery of molecules to plasmonic nanofocusing SERS structures. Nat. Photonics. 2011; 5:682–687.

197. Gentile F, Coluccio ML, Coppedè N, Mecarini F, Das G, Liberale C, et al. Superhydrophobic Surfaces as Smart Platforms for the Analysis of Diluted Biological Solutions. ACS Appl. Mater. Interfaces. 2012; 4:3213–3224. [PubMed: 22620470]

198. De Ninno A, Ciasca G, Gerardino A, Calandrini E, Papi M, De Spirito M, et al. An integrated superhydrophobic-plasmonic biosensor for mid-infrared protein detection at the femtomole level. Phys. Chem. Chem. Phys. 2015; 17:21337–21342. [PubMed: 25712032]

199. McLane J, Wu C, Khine M. Enhanced Detection of Protein in Urine by Droplet Evaporation on a Superhydrophobic Plastic. Adv. Mater. Interfaces. 2014; 2

200. Falde EJ, Yohe ST, Grinstaff MW. Surface Tension Triggered Wetting and Point of Care Sensor Design. Adv. Healthc. Mater. 2015; 4:1654–1657. [PubMed: 26097150]

201. Qing G, Wang X, Jiang L, Fuchs H, Sun T. Saccharide-sensitive wettability switching on a smart polymer surface. Soft Matter. 2009; 5:2759–2765.

202. Qing G, Sun T. Chirality-triggered wettability switching on a smart polymer surface. Adv. Mater. 2011; 23:1615–1620. [PubMed: 21472788]

203. Qing G, Wang X, Fuchs H, Sun T. Nucleotide-responsive wettability on a smart polymer surface. J. Am. Chem. Soc. 2009; 131:8370–8371. [PubMed: 19492797]

204. Ueda E, Levkin PA. Emerging Applications of Superhydrophilic-Superhydrophobic Micropatterns. Adv. Mater. 2013; 25:1234–1247. [PubMed: 23345109]

205. Neto AI, Custódio CA, Song W, Mano JF. High-throughput evaluation of interactions between biomaterials, proteins and cells using patterned superhydrophobic substrates. Soft Matter. 2011; 7:4147–4151.

206. Geyer FL, Ueda E, Liebel U, Grau N, Levkin PA. Superhydrophobic–Superhydrophilic Micropatterning: Towards Genome-on-a-Chip Cell Microarrays. Angew. Chemie Int. Ed. 2011; 50:8424–8427.

207. Shiu JY, Kuo CW, Whang WT, Chen P. Addressable cell microarrays via switchable superhydrophobic surfaces. J. Adhes. Sci. Technol. 2010; 24:1023–1030.

208. Wolinsky JB, Colson YL, Grinstaff MW. Local drug delivery strategies for cancer treatment: Gels, nanoparticles, polymeric films, rods, and wafers. J. Control. Release. 2012; 159:14–26. [PubMed: 22154931]

209. Allen TM, Cullis PR. Liposomal drug delivery systems: From concept to clinical applications. Adv. Drug Delivery Rev. 2013; 65:36–48.

210. Mura S, Nicolas J, Couvreur P. Stimuli-responsive nanocarriers for drug delivery. Nat. Mater. 2013; 12:991–1003. [PubMed: 24150417]

211. Kraft JC, Freeling JP, Wang Z, Ho RJY. Emerging research and clinical development trends of liposome and lipid nanoparticle drug delivery systems. J. Pharm. Sci. 2014; 103:29–52. [PubMed: 24338748]

212. Kesharwani P, Jain K, Jain NK. Dendrimer as nanocarrier for drug delivery. Prog. Polym. Sci. 2014; 39:268–307.

213. Lima AC, Song W, Blanco-Fernandez B, Alvarez-Lorenzo C, Mano JF. Synthesis of temperature-responsive dextran-MA/PNIPAAm particles for controlled drug delivery using superhydrophobic surfaces. Pharm. Res. 2011; 28:1294–1305. [PubMed: 21298327]

214. Lima AC, Mano JF, Concheiro A, Alvarez-Lorenzo C. Fast and Mild Strategy, Using Superhydrophobic Surfaces, to Produce Collagen/Platelet Lysate Gel Beads for Skin Regeneration. Stem Cell Rev. Reports. 2015; 11:161–179.

215. Hu X, Liu S, Zhou G, Huang Y, Xie Z, Jing X. Electrospinning of polymeric nanofibers for drug delivery applications. J. Control. Release. 2014; 185:12–21. [PubMed: 24768792]

216. Chou SF, Carson D, Woodrow KA. Current strategies for sustaining drug release from electrospun nanofibers. J. Control. Release. 2015; 220:584–591. [PubMed: 26363300]
217. Yohe ST, Freedman JD, Falde EJ, Colson YL, Grinstaff MW. A Mechanistic Study of Wetting Superhydrophobic Porous 3D Meshes. Adv. Funct. Mater. 2013; 23:3628–3637.. [PubMed: 25309305]
218. Kaplan J, Grinstaff M. Fabricating Superhydrophobic Polymeric Materials for Biomedical Applications. J. Vis. Exp. 2015:1–e53117.
219. Yohe ST, Kopechek JA, Porter TM, Colson YL, Grinstaff MW. Triggered Drug Release from Superhydrophobic Meshes using High Intensity Focused Ultrasound. Adv. Healthc. Mater. 2013
220. Manna U, Kratochvil MJ, Lynn DM. Superhydrophobic Polymer Multilayers that Promote the Extended, Long-Term Release of Embedded Water-Soluble Agents. Adv. Mater. 2013; 25:6405–6409. [PubMed: 23983053]
221. Kaplan JA, Liu R, Freedman JD, Padera R, Schwartz J, Colson YL, et al. Prevention of lung cancer recurrence using cisplatin-loaded superhydrophobic nanofiber meshes. Biomaterials. 2016; 76:273–281. [PubMed: 26547283]
222. Wang J, Kaplan JA, Colson YL, Grinstaff MW. Stretch-Induced Drug Delivery from Superhydrophobic Polymer Composites: Use of Crack Propagation Failure Modes for Controlling Release Rates. Angew. Chemie Int. Ed. 2016; 55:2796–2800.
223. Zhao Y, Zhu Y. Synergistic cytotoxicity of low-energy ultrasound and innovative mesoporous silica-based sensitive nanoagents. J. Mater. Sci. 2014; 49:3665–3673.
224. Ahmad Nor Y, Niu Y, Karmakar S, Zhou L, Xu C, Zhang J, et al. Shaping Nanoparticles with Hydrophilic Compositions and Hydrophobic Properties as Nanocarriers for Antibiotic Delivery. ACS Cent. Sci. 2015; 1:328–334. [PubMed: 27162988]
225. Yildirim A, Chattaraj R, Blum NT, Goldscheitter GM, Goodwin AP. Stable Encapsulation of Air in Mesoporous Silica Nanoparticles: Fluorocarbon-Free Nanoscale Ultrasound Contrast Agents. Adv. Healthc. Mater. 2016; 5:1290–1298. [PubMed: 26990167]
226. Chen L, Wang W, Su B, Wen Y, Li C, Zhou Y, et al. A light-responsive release platform by controlling the wetting behavior of hydrophobic surface. ACS Nano. 2014; 8:744–751. [PubMed: 24383581]
227. Tuteja A, Choi W, Mabry JM, McKinley GH, Cohen RE. Robust omniphobic surfaces. Proc. Natl. Acad. Sci. 2008; 105:18205–19200.
228. Rawal A. Design Parameters for a Robust Superhydrophobic Electrospun Nonwoven Mat. Langmuir. 2012; 28:3285–3289. [PubMed: 22251513]
229. Kleingartner JA, Srinivasan S, Truong QT, Sieber M, Cohen RE, Mckinley GH. Designing Robust Hierarchically Textured Oleophobic Fabrics. Langmuir. 2015; 31:13201–13213. [PubMed: 26473386]
230. Cytonix LLC. Fluorothane™. 2016. (2014), doi:http://www.cytonix.com/fluorothane.html
231. Farhangi MM, Graham PJ, Choudhury NR, Dolatabadi A. Induced Detachment of Coalescing Droplets on Superhydrophobic Surfaces. Langmuir. 2011; 28:1290–1303.

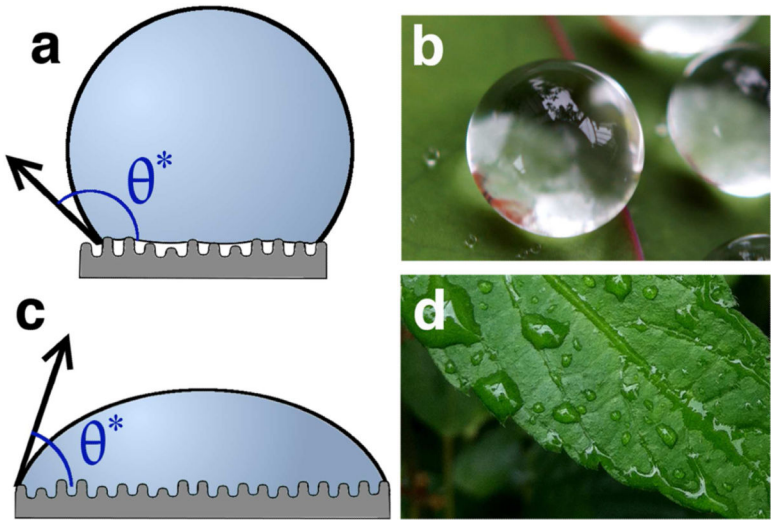

Figure 1.

Diagram of wetting states on rough materials and examples in nature. **a)** The Cassie-Baxter (CB) partially wetted state and **c)** the Wenzel complete wetting state. Examples of natural materials are **b)** lotus leaves, which are the canonical example of a natural superhydrophobic material, and **d)** the hydrophilic leaves of petunias in genus *Ruellia*. Photos are courtesy of Takashi Matsuzawa and Mark Swanson.

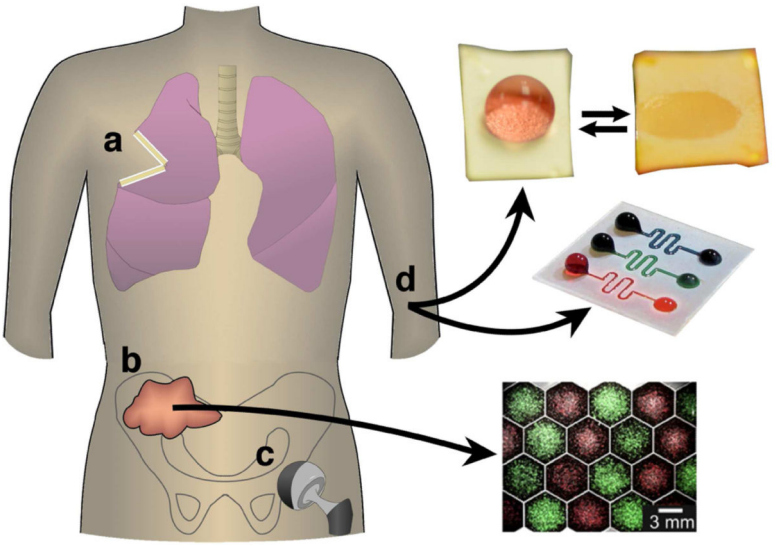

Figure 2.

Superhydrophobic materials are of interest for a variety of medical applications including: **a)** control of the local release of drugs after tumor resection, **b)** patterned cell growth to study cellular communication (i.e., from a biopsy), **c)** reduced bacterial adhesion on implants such as hip replacements, or **d)** stabilization of droplets or drive flow in microfluidics and diagnostic assays. Photos are adapted with permission from [190] and [146].

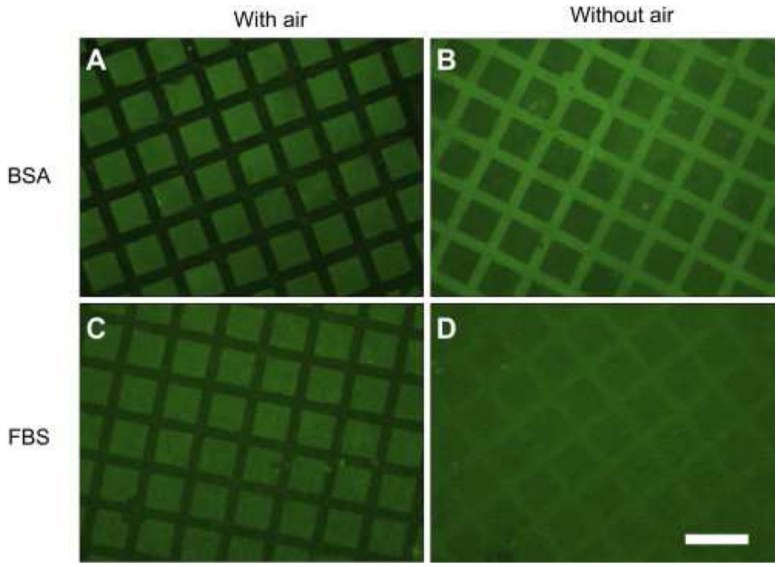

Figure 3.

Entrapped air at the superhydrophobic surface prevents protein binding (protein is shown in green) when incubated both with BSA or FBS (A,C). Removal of the air layer through sonication leads to protein binding in the regions that were once protected (B,D). Figure is reprinted with permission from [129].

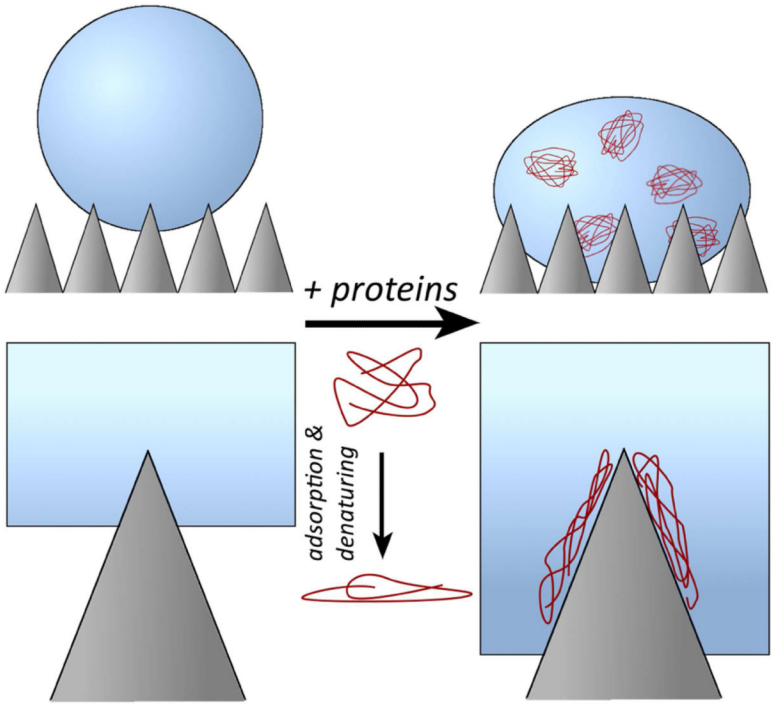

Figure 4.

Illustration of how protein fouling (biofouling) of superhydrophobic surfaces may lead to removal of the air layer. Proteins denature at the superhydrophobic/hydrophobic surface, leading to proteins binding and subsequent surface wetting due to formation of a more hydrophilic interface.

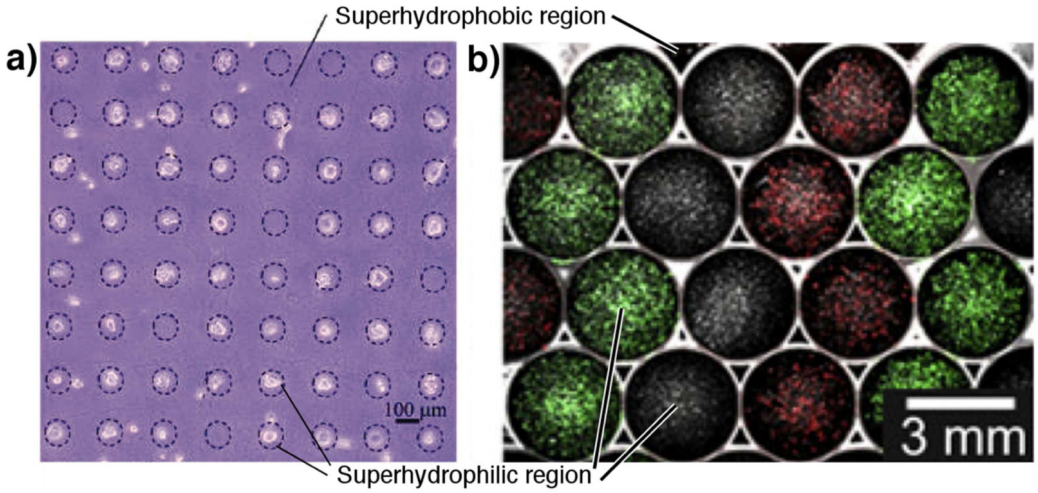

Figure 5.

Superhydrophobic regions prevent cellular binding and growth, where superhydrophilic regions showed the opposite. **a)** Minimal binding of cells on superhydrophobic regions occurs while significant adhesion occurs on superhydrophilic surfaces, adapted with permission from [144]. **b)** Adjacent superhydrophilic spots can be seeded with droplets of different cell populations separated by superhydrophobic barriers, after which the entire surface can be wetted to study cell-cell communication, adapted with permission from [146].

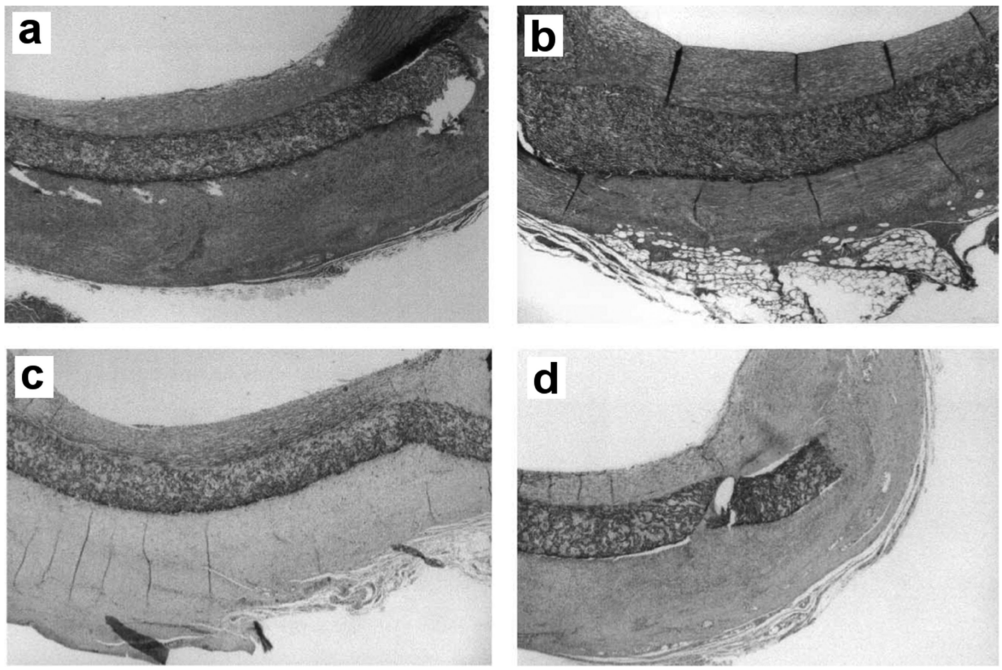

Figure 6.

(a) Standard hydrophobic ePTFE and (b) superhydrophobic PTFE showed no difference in neointima formation on the luminal side of the patch in a pig carotid circulation model after 4 weeks. No thrombus formation was observed. As shown by α-actin staining, the majority of neointima formation in (c) ePTFE and (d) superhydrophobic PTFE is smooth muscle, reprinted with permission from [155].

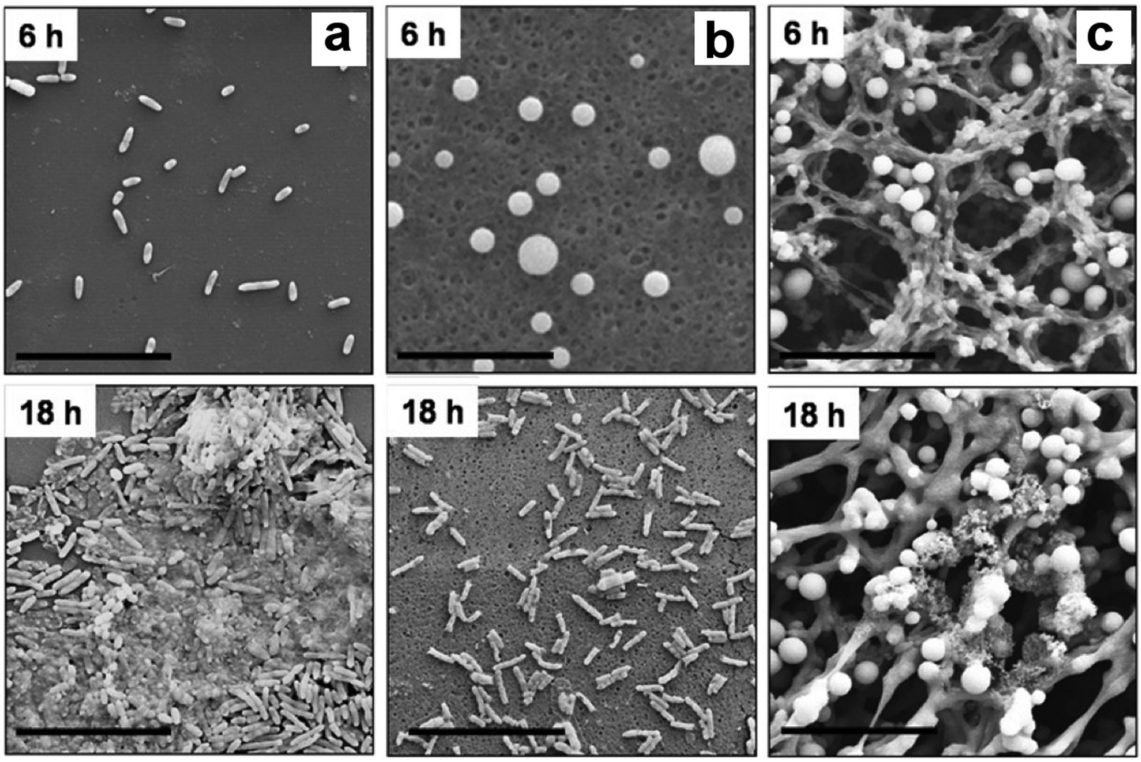

Figure 7.

SEM images of *P. aeruginosa* PAO1 colonization on hydrophobic **(a)** and two types of superhydrophobic **(b) (c)** surfaces after 6 and 18 hours of incubation. Colonization occurred more slowly with a more stable superhydrophobic state (**a**→**b**). Figure adapted with permission from [170].

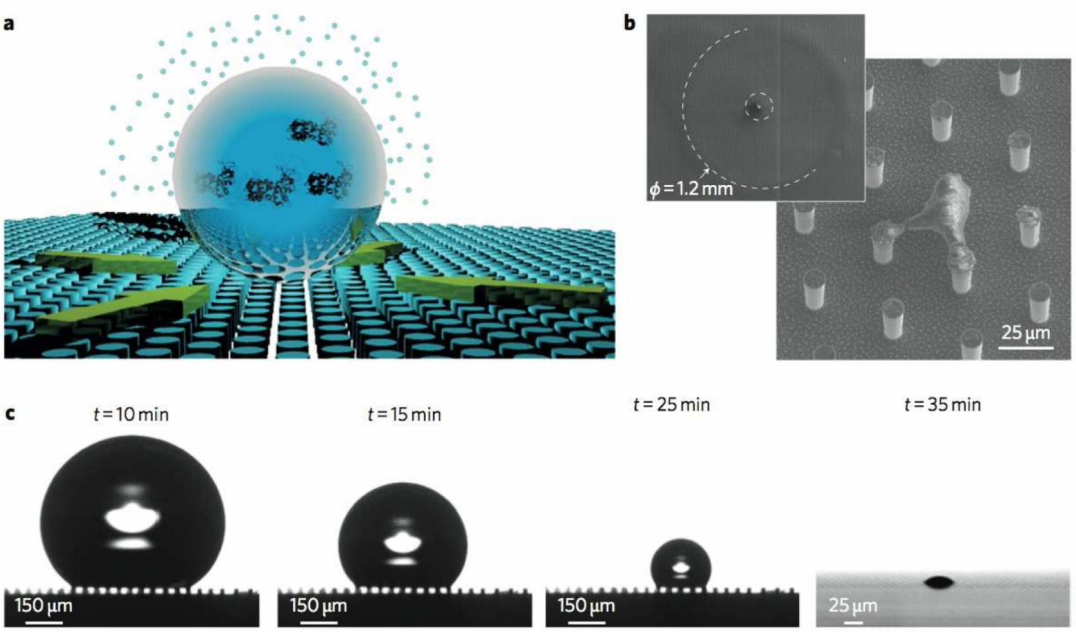

Figure 8.

Superhydrophobic surfaces allow deposition of molecules on a small number of pillars during evaporation (a, b, c). Concentration of non-volatile components at pillars allows detection of femto- to attomolar concentrations of biomolecules with an appropriate plasmonic structure on the pillars. Adapted with permission from [196].

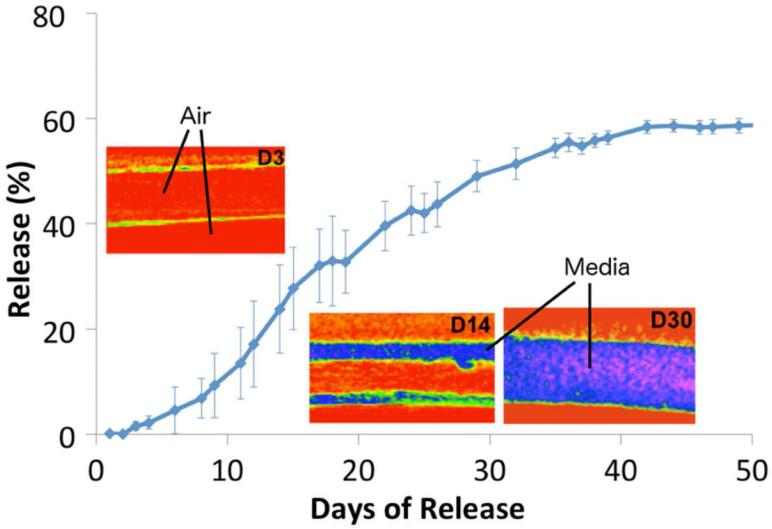

Figure 9.

The removal of air from superhydrophobic 3D materials controls the rate of drug release from the central layer of a tri-layered electrospun mesh. Each layer of an electrospun mesh acts as a new superhydrophobic surface to control the rate of air removal and penetration of a serum solution, imaged using μCT with a contrast agent. Figure adapted from [78].